



FLORIDA SOLAR ENERGY CENTER®

Creating Energy Independence

Side-by-Side Testing of Water Heating Systems: Results from the 2009-2010 Evaluation

FSEC-CR-1856-10

June 2010

Submitted to

U.S. Department of Energy

DOE Award No. DE-FC26-06NT42767

UCF/FSEC Contract No. 20126034

Author

Carlos J. Colon

Danny S. Parker

Copyright ©2009 Florida Solar Energy Center/University of Central Florida
All Rights Reserved.

1679 Clearlake Road
Cocoa, Florida 32922, USA
(321) 638-1000

www.floridaenergycenter.org



A Research Institute of the University of Central Florida

Disclaimers

This report was prepared as an account of work sponsored by an agency of the United States government. Neither the United States government nor any agency thereof, nor any of their employees, makes any warranty, express or implied, or assumes any legal liability or responsibility for the accuracy, completeness, or usefulness of any information, apparatus, product, or process disclosed, or represents that its use would not infringe privately owned rights. Reference herein to any specific commercial product, process, or service by trade name, trademark, manufacturer, or otherwise does not necessarily constitute or imply its endorsement, recommendation, or favoring by the United States government or any agency thereof. The views and opinions of authors expressed herein do not necessarily state or reflect those of the United States government or any agency thereof.

Acknowledgements

This work is sponsored by the U.S. Department of Energy (DOE), Office of Energy Efficiency and Renewable Energy, Building America Program under cooperative agreement number DE-FC26-06NT42767. The support and encouragement of program managers ó Mr. George James, Mr. Terry Logee, Mr. Ed Pollock and Mr. William Haslebacher ó is gratefully acknowledged. This support does not constitute DOE endorsement of the views expressed in this report.

The authors appreciate the support of Rob Vieira and Subrato Chandra for their suggestions in the preparation of this report. We also appreciate the editorial assistance from Danielle R. Daniel.

Table of Contents

Executive Summary	1
Testing Plan, Hot Water Draw Schedule and Initial Results	2
Impact of Pipe Insulation	3
Summary of First Year Results	4
Daily Electricity Savings	5
Time-of-Day Load Shape Impacts	5
Introduction	8
Objectives	8
HWS Facility Description.....	8
Instrumentation and Controls.....	10
Hot Water Systems Selection.....	11
Test Configurations	11
1. Standard 50-gallon electric water heater (electric baseline reference)	12
2. Flat Plate Solar System Differentially Controlled, with 80-gallon storage tank.....	12
3. Integrated Collector System (32 ft ²) in series with Std. electric 50-gallon.....	12
4. Solar Flat Plate System with photovoltaic (PV) DC pump with 80-gallon storage	13
5. Gas Water Heater ó Standard Residential 40-gallon.....	13
6. Tankless Gas Heater.....	13
7. Tankless Electric Heater.....	13
Testing of 10 W Photovoltaic Module	13
Test Protocols and Established Draws.....	14
Seasonality of Water Heating Loads: Inlet Water Temperature Variation.....	14
Seasonal Variation in Florida Hot Water Use	16
Hot Water Supply Temperature	19
Tankless Electric System	20
Experimental Log	21
Analysis and Results	21
Evaluation of Impact of Pipe Insulation During Shakedown	21
Summary of Results.....	22
Daily Electric Consumption.....	25
Time of day Electric Demand	25
Summer and Winter Peak Day Analysis.....	27
Summer Peak Hour (June 22, 2009, 5:00 PM).....	27
Winter Peak Hour (January 11, 2010, 8:00 AM)	28

Table of Contents (cont)

Impact of Raw Profile and on Seasonal Efficiency	28
Reference Standard Electric 50 Gallon Tank.....	28
Tankless Electric	29
Natural Gas 40 Gallon Storage Tank.....	29
Tankless Natural Gas	30
Flat plate Solar Systems.....	30
ICS Simulation Efforts	31
SDHW Tool (TRNSYS) Simulations Against Measured Data.....	31
Heat Loss Investigation on ICS Model.....	32
Influences on Efficiency	33
Recommendations for Follow-up Testing	34
Conclusions and Recommendations	34
New Draw Profile (NREL/BA) and Influence on Efficiencies.....	35
Average Daily Performance.....	36
References	40
Appendix A.....	42

Side-by-Side Testing of Water Heating Systems: Results from the 2009-2010 Evaluation

Carlos J. Colon and Danny S. Parker

Florida Solar Energy Center

June 2010

Executive Summary

The performance of seven differing types of residential water heating systems was compared in a side-by-side test configuration over a full year period. The Hot Water System Laboratory (HWS Lab) test facility at the Florida Solar Energy Center (FSEC) in Cocoa, FL was used for the tests. Simultaneous hot water draws occur on a daily basis for the following hot water heating systems at the HWS facility with the evaluation of two draw profiles:

- Standard electric resistance 50-gallon tank
- Solar flat plate collector (40 ft²) connected to an 80-gallon storage tank with temperature differential controlled pump ó direct loop circulation
- Integrated Collector System (ICS, 32 ft²) connected to a standard 50-gallon water heater
- Solar Flat Plate collector (40 ft²) connected to an 80-gallon storage tank with photovoltaic pump ó direct loop circulation
- Standard residential 40-gallon natural gas water heater tank (storage upright vented type)
- Natural Gas tankless water heater
- Electric tankless water heater



Figure E-1. HWS Lab at Florida Solar Energy Center with collector roof stands.

Three of the seven are FSEC certified solar systems of the most common residential type installed in the state of Florida. All are direct open-loop type and unsuitable for freezing climates. A standard 50-gallon residential water heater with an energy factor (EF) rating of 0.91 is used as baseline. Similarly, the differential controlled flat plate system is also considered a reference solar system and will remain as baseline in future testing. Although testing began during February 2009, March 1st is considered the official starting date where all adjustments to the controls and data acquisition were finalized. Since the end of February 2010, the HWS

Laboratory has collected twelve months of data which is stored in our data base system (*GET v. 4.0*) and is easily accessed through our www.infomonitors/HWS website.

The website default page displays a summary report of the previous days' data and provides a link access to over 90 channels of detailed data. In addition to displaying energy values and gallons used, the report format also summarizes draw-weighted inlet and outlet temperature averages and daily system efficiencies.

Testing Plan, Hot Water Draw Schedule and Initial Results

During the summer of 2008, a consensus-based Building America (BA) analysis was performed to determine a suitable hot water draw pattern for realistic testing of residential water heating systems (Hendron and Burch, 2007). In consultation with the National Renewable Energy Laboratory (NREL), a decision was made to alternate between ASHRAE 90.2 and a dynamic monthly draw schedule that better represented typical family hot water usage. A new hot water draw schedule was created, which we refer to as the NREL/BA draw profile. The average daily hot water draw was 54.8 gallons/day.

The new draw profile was developed from Building America source documentation with the addition of monthly changes in hot water loads. The decision to adjust the quantity of daily hot water draws on a monthly basis, as shown in Table E-1, was attributable to the magnitude of mains inlet temperature variations observed in central Florida throughout the year. Specific earlier monitoring of hot water use in Florida homes showed levels of volume related, seasonal changes and also formed a basis for this assessment (Merrigan, 1988).

Current data from our monitoring in February 2009 thru March 2010 reveals an inlet water temperature trend, as shown in Figure E-2. Mains water inlet temperatures were measured to vary by nearly 34°F from the lowest to highest month. Incidentally, the plot also shows the ability of an integrated collector system (ICS) to increase water temperatures prior to reaching the auxiliary storage water heater tank.

Table E-1
NREL/BA Draw Schedule

Month	NREL/BA Schedule Daily Hot Water Draw (gallons)
January	67.2 (max. draw)
February	66.4
March	66.4
April	63.8
May	54.6
June	48.4
July	42.2 (min. draw)
August	44.0
September	44.9
October	47.5
November	53.7
December	59.0
Average	54.8

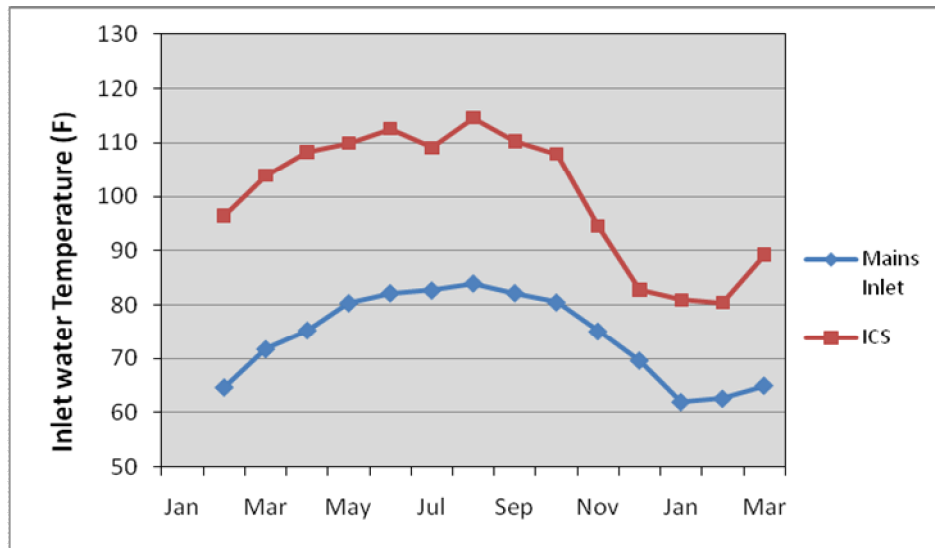


Figure E-2. Average inlet water temperature by month for the standard electric mains inlet and those provided by an ICS system.

The NREL/BA draw profile was implemented for testing at the HWS Lab during the latter part of May 2009. Rotations between the two draw schedules were carried every two weeks each month. As a result, data presented in the report includes over 12 months of data, completing the dual-profile testing period at the end of April 30, 2010. The NREL/BA draw schedule represents a more realistic family draw pattern (with multiple events each hour) as opposed to the hourly events adopted in ASHRAE 90.2 with an unvarying 64.3 gallons per day throughout the year.

Impact of Pipe Insulation

From March 3 thru March 10, 2009, during the facility experimental shakedown, we applied foam insulation (R-2) to all exposed piping located inside the HWS building. IR thermograph showed significant losses prior to insulation (Figure E-3). An evaluation of the impact of piping insulation was performed for similar matched days (insolation and temperature) prior to and after insulation. We found a dramatic impact on the two solar systems which circulated during the day.

- The average daily COP of the flat plate differential system increased from 5.54 to 8.30, corresponding to an increase in solar fraction of approximately 3%.
- The average daily COP of the more slowly pumped, flat plate PV system increased from 3.69 to 6.06, an increase in solar fraction by approximately 10%.
- The average daily COP of the ICS system increased from 1.86 to 2.12, an increase in solar fraction by approximately 7%.



Figure E-3. Visible and infrared image of piping heat losses prior to insulation.

Thus, the data shows during February/March conditions that pipe insulation exerts between a 5 and 10% influence on achieved solar fraction ó highly significant given its low cost. We conclude that improvements to pipe insulation technology could provide significant improvements to solar system performance, particularly under winter conditions.

Summary of First Year Results

Between the period of March 1 and February 2009, the overall combined average daily efficiency using both *ASHRAE 90.2* and NREL/BA hot water draw schedules is shown in Figure E-4. Parasitic energy is included in the calculations for the two systems that have auxiliary energy requirements: the controllers in the natural gas tankless and the differential activated pump in the solar system. Results from testing indicate that daily efficiencies for these systems are generally below the published energy factor ratings (which are shown in brackets).

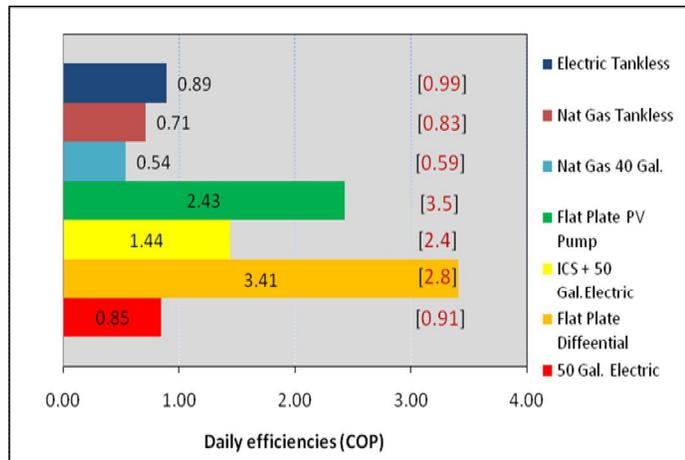


Figure E-4. Comparative average COP of tested systems over twelve month period [Nominal EF in brackets].

The differential flat plate solar systems demonstrated higher efficiencies than its solar energy factor rating. The PV pumped system also yielded very good performance. As expected, these solar systems surpass the other types regardless of hot water draw schedule. The highest average daily efficiency for this period (COP = 3.41) was demonstrated by the flat plate solar system, which utilizes a differential controller and AC pump. During the first eight months of testing, the PV-pump system had demonstrated the highest overall efficiencies. However, during cloudy days and winter period, the differential-controlled flat-plate solar system exceeded the efficiency of the PV-pumped system likely due to its better circulation flow rate. This finding suggests that a larger photovoltaic module might improve efficiency for the PV-circulated solar system during cooler cloudy weather.

One of the reasons for the lower than expected baseline electric system efficiency is the reduced volume of hot water utilized under the NREL/BA hot water schedule. This lower consumption, along with higher inlet water temperatures in Florida, reduces the amount of energy provided during summer draws. Thus, standby losses become a higher percentage of energy use as compared to the total energy delivered, yielding lower daily efficiencies (Figure E-5).

Daily Electricity Savings

Daily electric consumption for five electric systems is compared in Figure E-6 for the period of May 2009 through April 2010. A complete one-year data set was recorded with both alternate draws. The plot indicates a 0.3 kWh average daily reduction for the tankless electric when compared to the standard electric baseline system. Solar thermal systems clearly demonstrate large daily electric reductions of between 5.5 and 3.5 kWh/day. The ICS system saves about 2.5 kWh/day.

Time-of-Day Load Shape Impacts

Electric demand for five systems was also analyzed for the total period to determine impact on time-of-day water heating load shape from 15-minute data. Figure E-7 reveals a peak load reduction demonstrated by flat plate (FP) solar systems when compared to the standard baseline electric (E50) particularly during the critical 7-8 AM hour. Data consists of the 24-hour average demand when evaluated from May 2009 thru April 2010. Morning peak demand reduction (8:00 AM) by the two solar flat-plate systems appears to be reduced on average

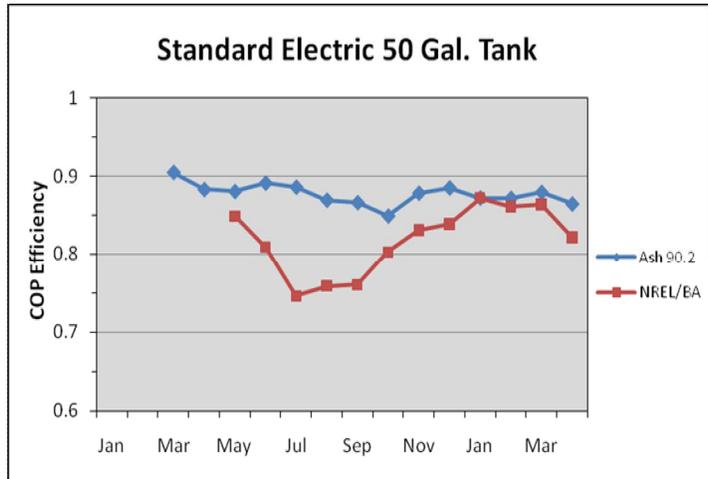


Figure E-5. Efficiency results obtained from the baseline electric 50-gallon water heater under *ASHRAE 90.2* and NREL/BA draw schedules

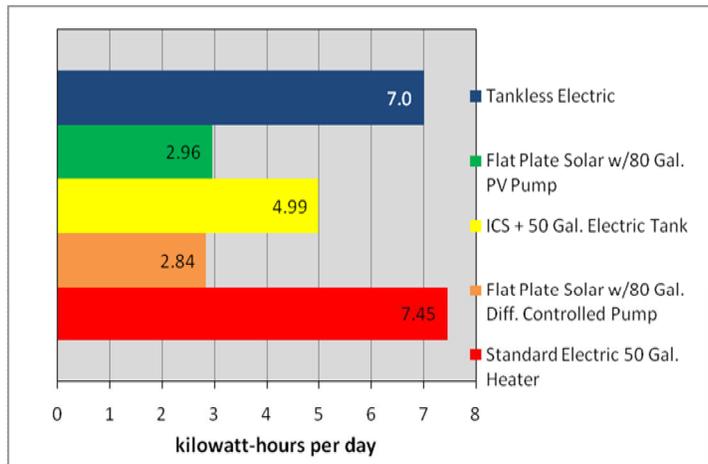


Figure E-6. Daily average electricity used for heating water measured from combined draw profiles.

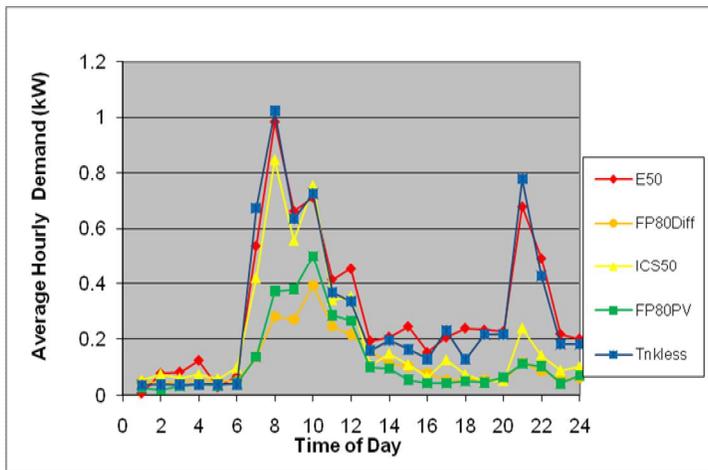


Figure E-7. Time of day electric demand for five water heating systems.

by 67%. The flat-plate solar systems appear to have shifted the peak by two hours (10:00 AM). Peak reduction at 8:00 AM by the ICS-50 solar system amounts to only 14%.¹

Draw Schedule Dependent Results

During May 2009, the HWS laboratory began alternate 2-week testing for each of the hot water profiles. Further analysis on distinctive data by draw pattern was performed to determine the average daily energy consumption by draw pattern. The results can be examined in Table E-2 which includes all data for 365 days and a breakdown analysis.

Table E-2
Results for May 2009 thru April 2010 Testing

System	Daily Average Consumption All data days (N=365)	Daily Average Consumption ASHRAE 90.2 Draws (N=166)	Daily Average Consumption NREL/BA Draws (N=174)
Standard Electric 50 gal. Tank	7.45 kWh/day	7.88 kWh/day	7.07 kWh/day
Solar Flat Plate Differential w/80 gal. tank	2.84 kWh/day	2.94 kWh/day	2.74 kWh/day
ICS w /50 gal. tank	4.99 kWh/day	4.79 kWh/day	5.21 kWh/day
Solar Flat Plate PV pumped w/80 gal.	2.96 kWh/day	3.09 kWh/day	2.87 kWh/day
Tankless Electric	7.00 kWh/day	7.34 kWh/day	6.71 kWh/day
Nat. Gas 40 gal. tank	39.08 cu. ft/day (Nat. Gas)	39.95 cu. ft/day (Nat. Gas)	38.32 cu. ft/day (Nat. Gas)
Tankless Nat. Gas	29.2 cu. ft/day (Nat. Gas)	30.56 cu. ft/day (Nat. Gas)	28.01 cu. ft/day (Nat. Gas)

Table E-3 shows the difference or change between ASHRAE 90.2 and NREL/BA draw schedules. Most systems see lower performance with the NREL/BA profile. The negative impact is most pronounced on the ICS system since ICS systems work best in summer when water heating loads are lower and more poorly in winter when water heating loads are larger. The NREL/BA profile, on the other hand, correctly reflects the fact that winter water heating loads are greater than those in the rest of the year.

Table E-3
Hot Water Electricity Savings by Technology and Draw Profile

	ASHRAE 90.2	NREL/BA	Change
Solar Flat Plate Differential w/80 gal. tank	62.7%	61.2%	-1.5%
ICS w /50 gal. tank	39.2%	26.3%	-13.0%
Solar Flat Plate PV pumped w/80 gal. tank	60.7%	59.4%	-1.4%
Tankless Electric	6.9%	5.0%	-1.9%

¹ It must be emphasized that peak impacts will be influenced by the time period chosen for the data aggregation and available data relative to weather. Thus, the impacts of the tankless electric system may be greater when the data is averaged on a 15-min. basis, or even on a 5-min. basis.

The tankless natural gas system reduced gas consumption by roughly 25% compared to the standard natural gas storage water heater. In this case, the tankless natural gas system demonstrated a slight energy reduction under the NREL/BA draw profile.

Table E-4
Hot Water Natural Gas Savings by Draw Profile

	ASHRAE 90.2	NREL/BA	Change
Tankless Nat. Gas	23.5%	26.9%	+3.4

In examining the results, we find that the energy use associated with the more realistic NREL/BA profile for a standard electric resistance water heater (7.07 kWh/day or 2,580 kWh/yr) closely compares to what FSEC measured in 150 electric resistance heaters in 1999 with *Progress Energy* (2,325 kWh) (Masiello and Parker, 2004).

Summarizing the annual reductions for the systems using the more realistic BA profile:

- Flat plate solar systems with either differential control or PV pumping saved 61% and 59% of baseline energy, respectively;
- ICS system saved 26% of water heating energy;
- Tankless electric saved only 5% of water heating energy;
- Tankless gas saved 27% of energy relative to a standard natural gas storage system.

Detailed findings from our research:

- The PV flat plate system does not appear to be circulating enough on cloudy days and thus efficiency suffers, particularly in winter. This issue will be researched in 2010-2011 with an augmented PV array for more pumping.
- The ICS system shows less favorable results with the BA/NREL profile since more hot water is needed in winter and less in summer; however, performance of the ICS system is worse in winter and better in summer. Consequently, the percent of electrical reduction is 39% for an ICS system with the 90.2 profile and only 26% with the BA/NREL profile.

Our research has also allowed insight into why TRNSYS has been over-predicting ICS performance relative to field studies. This question likely arises because ICS system performance is strongly impacted by a seasonally weighted hot water draw profile. However, our research indicates that the BA/NREL profile is generally more realistic relative to monitored data and better reflects the typical homeowner conditions.

Introduction

With increased emphasis on reducing residential energy use and on higher federal, state and local utility incentives, solar water heaters are once again being installed in significant numbers across the nation. Solar thermal water heating is an excellent way to save on whole house energy to meet the U.S. DOE Building America (BA) program goals for Zero Energy Homes. To compare the performance of different types of solar and conventional water heaters, a test facility was constructed at the Florida Solar Energy Center (FSEC) in Cocoa, FL. The facility allows testing of seven systems simultaneously in a side-by-side configuration and the ability to evaluate different water draw schedules.

Objectives

The objective of the water heating systems evaluation project is to compare energy performance and time-of-day electric loads by conducting side-by-side tests of solar and conventional domestic hot water (DHW) systems. Additionally, results from testing will help enhance and validate simulation models for water heating systems, especially solar integrated collector and storage (ICS) systems. Ultimately, the project is to analyze the overall status of water heating equipment in the U.S. and to encourage future system designs that improve efficiency.

HWS Facility Description

The Hot Water System (HWS) Laboratory at the Florida Solar Energy Center (FSEC) in Cocoa, FL, is a 10-ft by 16-ft factory built test structure. The shed-type building features a white metal hip roof, an un-insulated open truss roof and plywood walls with exterior vinyl siding. The building has an east facing window and double entry doors with a partial glass area facing north. The HWS facility was installed on FSEC premises (Figure 1) and is set apart at 23 feet from steel rails which serve as stands for various tested solar systems. Two partial roof structures, each with enough area to install two 4-ft by 10-in. collectors were constructed on site to serve as residential platforms for the solar thermal systems. These platforms simulate a residential roof structure with three-dimensional tab shingles (dark brown) on a 5/12 (22 degree) pitch roof. The roof color and inclination were selected to be representative of the most common roof type and slope in the residential building stock.



Figure 1. HWS Laboratory at the Florida Solar Energy Center, Cocoa, FL.

The size of the building was chosen to contain five hot water storage tanks and two tankless systems, as shown in the layout of Figure 2.

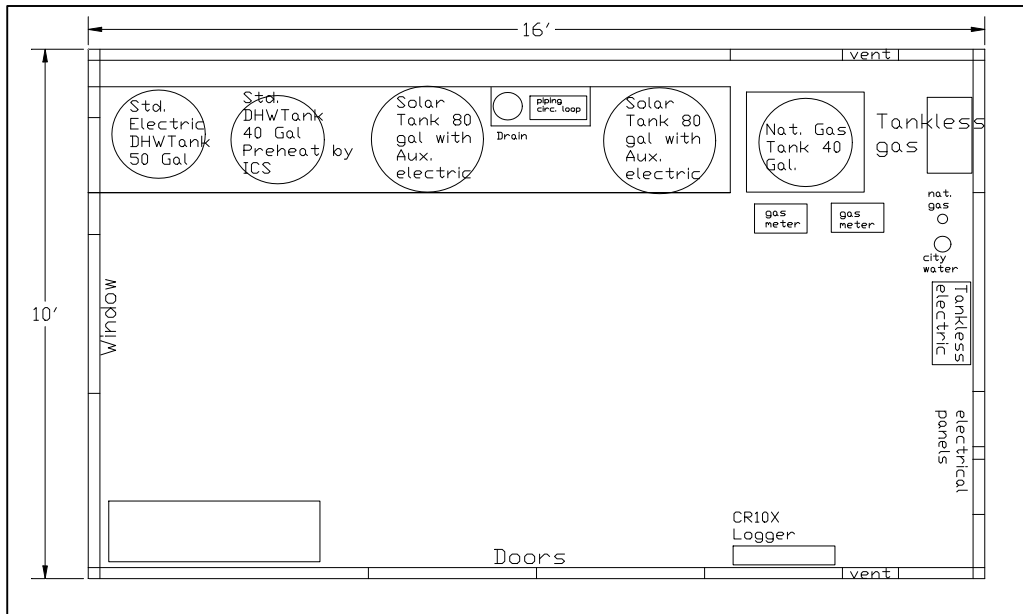


Figure 2: Schematic layout of hot water tanks and hot water heating systems at FSEC's HWS laboratory.

The HWS building sits on pressure-treated footers spaced 16 inches on-center and features a pressure treated wood floor system. Three of the systems with tank storage are connected to solar thermal collectors, the other two being a reference baseline 50-gallon electric water heater and a 40-gallon natural gas tank water heater. The remaining two systems are tankless, one being natural gas and the other a tankless electric with multiple electric resistance heating elements (22 kW maximum).

A $\frac{3}{4}$ inch gas line sized to two-inch water columns (i.w.c.) of gas pressure capacity over 140 ft. in length was installed to provide natural gas to the standard 40-gallon tank and residential tankless system. A fourteen i.w.c. pressure-reducing valve was installed at the service meter supplying the gas operating service typical for this region in Florida. However, pressure was reduced further to 10.0 i.w.c. to each gas appliance, respectively. (A maximum operating pressure of 10.5 i.w.c. is posted on the front plate of the tankless natural gas system.)

Additional vents were added to the north and south walls to comply with ventilation code for natural gas combustion appliances. Combustion exhaust for the tankless system was routed through the west wall. The 40-gallon gas water heater was vented through the metal roof using a standard three-inch vent and an exterior high temperature boot kit to seal against the metal roof.

The HWS structure is set off the ground with a 12-inch ground clearance. Water mains feed, natural gas lines, and all circulation pipes running from the HWS Lab to solar collector stands were routed underground. A $1\frac{1}{4}$ inch PVC mains water supply line was installed to the HWS Lab from FSEC's central energy plant. Circulation loops assembled with $\frac{1}{2}$ inch nominal outside diameter (OD) rigid copper tubing were soldered and installed underground. The lines were insulated with $\frac{1}{2}$ inch open cell insulation (R=2.0) and encased in $1\frac{1}{2}$ inch PVC tubing to

minimize heat losses and ground interaction. The longest circulation loop serves the solar thermal differential flat plate system. As a result, additional copper tubing was added to the second solar flat plate system (i.e., PV pumped) to bring the total circulation lengths to par. Table 1 is a summary of circulation loop and feed lines installed on the three solar collectors.

Table1
Length of Circulation Loops for Various Solar Systems at the HWS Laboratory

	Underground Insulated Piping (R = 2.0)	Lab and Stand Piping	Added Piping at Roof Stand	Total Circulation Loop (ft)
Differential controlled Flat Plate Solar(direct)	101.6 ft.	52.0 ft.	0.0	153.6 ft.
PV Pumped Flat Plate Solar (direct)	101.2 ft.	46.3 ft.	6.0	153.6 ft.
ICS	51.7 ft. (collector to tank only)	16.5 ft.	N/A	68.3ft.

No additional length was added to the ICS system since the ICS design does not rely on a circulation loop. The only disadvantage presented to the ICS is the length of 68.3 feet (½ inch type M copper) tubing from the ICS collector pre-feeding the storage tank. On short hot water draws, some of the pre-heated water would never reach the storage tank.

Based on the inside diameter of a Type M copper tubing (0.569 inch), the water in the lines to the ICS system would equate to about 0.8 gallons of hot water in transit between the collector and the 50-gallon electric tank. Depending on the timing of follow-up hot water draws, some or all of the heat might be dissipated through the pipe wall/insulation and lost into the ground.

To accommodate all power requirements, a 70 KVA transformer was installed to supply electrical energy to all systems. Two distribution panels were used in the electrical distribution. One of them was dedicated to the tankless electric heater which has a maximum power rating of 22 kW (91 amps @ 240 volts).

Instrumentation and Controls

The data acquisition system at the HWS Laboratory is programmed to sample data every 12 seconds and average integrated measurements every 15 minutes. At the data collection commencement on March 1, 2009, the ASHRAE 90.2 draw profile was exclusively used (Figure 3). All of the systems are simultaneously drawn to the profile in use at a flow rate of approximately 1.5 gpm.

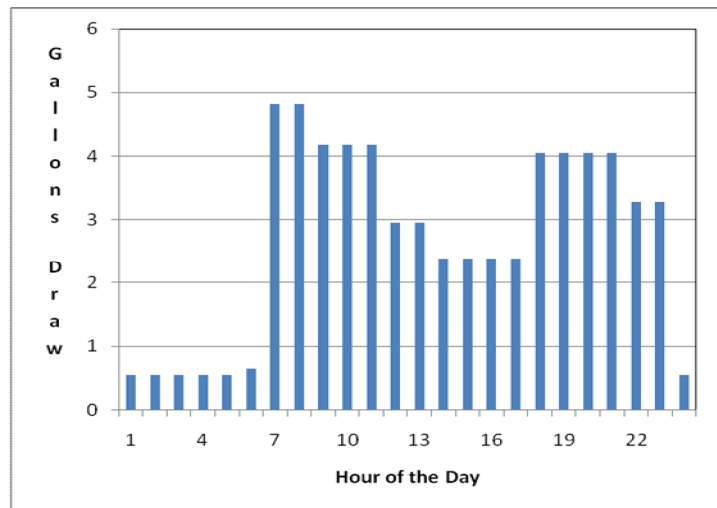


Figure 3. Hourly quantities of hot water gallons under ASHRAE 90.2 draw schedule.

However, beginning in May 2009, the controller was programmed every two weeks changing hot water draw profiles. Starting in May, every two weeks and thereof, draw profiles were adjusted, allowing data to gather under similar weather patterns. The second hot draw pattern used was the NREL/BA draw profile, which differs from the ASHRAE 90.2. The ASHRAE 90.2 draw profile executes draws every hour of the day (24 events) while the NREL/BA draw profile is more representative of a family use pattern. As a result, the latter does not draw during early hours of the day. The NREL/BA draw events can begin at any minute within the hour differing from the ASHRAE which draws at the beginning of every hour. Another marked difference is that the amount of hot water gallons drawn in the ASHRAE profile stays constant during the year (64.3 gallon per day) while the NREL/BA draw profile varies by month given the known seasonality in the quantity of residential hot water use. More information on the NREL/BA draw schedule is discussed in Test Protocol and Established Draws section.

Hot Water Systems Selection

Selection of hot water heating systems was made to reflect the most common residential models used in central and south Florida (non-freeze areas) that were available in the market for each category. Consultation with the industry (Rheem) and through FSEC solar thermal division occurred prior to purchasing the systems. Final selection resulted in five systems with storage tanks and two tankless systems. Three of the systems selected are of solar thermal design plumbed to their appropriate storage tank size. Two of the systems operated on natural gas, one standard residential 40-gallon tank and one of tankless design.

Table 2 presents a general description of all seven systems used for testing in 2009 including the published energy factor rating and model number.

Table 2
Hot Water System Description, Energy Factors and Model

Hot Water Heating System	Energy Factor	Manufacturer	Model
50-Gallon Standard Electric Tank	0.91	Rheem	50T06AAG
Flat Plate Solar Thermal w/80 gal. Storage, Differential Control	2.8 (FEF Central)	AET	D-80-40
ICS w/50 gal. Electric	2.4 (FEF)	TCT/Rheem	PT40 + 50T06AAG
Flat-Plate Solar Thermal w/80 gal. storage, PV Pumped	3.5 (FEF)	AET	DPV 80-40
50-Gallon Natural Gas Tank	0.59	GE	22V40F1
Tankless System - Natural Gas	0.83	Takagi	TK-3
Tankless Electric	0.99+	Seisco	RA-22

Test Configurations

Figure 4 shows a panoramic view of the inside layout of all tanks and water heating systems in the HWS laboratory. A brief test case description follows for the systems shown in the picture starting at left with the standard 50-gallon electric heater and the tankless electric shown in the picture below.



Figure 4. Hot water storage tanks and systems under testing at HWS laboratory.

1. Standard 50-gallon electric water heater (electric baseline reference)

This standard residential water heating system operates with one of two heating elements rated at 4500 watts. Three-quarter-inch type L copper tubing was used for the inlet and outlet connections. Thermostats were set to 120°F. This 50-gallon tank is our reference standard electric water heater.

Measurements for System 1
Tank Inlet water temp. (°F)
Tank outlet water temp. (°F)
Flow meter (gal.)
Tank Electric Element (kW)

2. Flat Plate Solar System Differentially Controlled, with 80-gallon storage tank

A differential controlled solar system AET D-80-40, is composed of an AE-40 Collector (4ø x 10ø), 80-gallon American Water Heater Co. (Model OST-80TCE) Storage Tank (59.25ø H x 24ø dia.), TACO 003-BC4 pump with differential temperature controller, and IMC Eagle I Plus, Single 4500W aux. heating element. Honeywell AM-101 mixing valve set to 120°F.

Measurements for System 2
Tank Inlet water temp. (°F)
Tank Outlet water temp. (°F)
Mixing valve outlet temp. (°F)
Solar collector Send (°F)
Solar collector Return (°F)
Inlet mains temp. (°F)
Flow meter (gal.)
Tank Electric Element (kW)

3. Integrated Collector System (32 ft²) in series with Std. electric 50-gallon

The ICS system is a PT40-CN (Thermal Conversion Technologies) Progressive Tube Collector (32.1 ft²) which holds 41.4 gallons. The ICS is plumbed in series to a standard 50-gallon tank acting as a pre-heater. As with all solar systems under test, a mixing valve was installed to the 50-gallon tank and set to 120°F. Upper and lower thermostats were also set to 120°F. Additional measurements were taken with a separate data logger to characterize temperature gradients inside the multi-tube integrated collector.

Measurements for System 3
Tank inlet water temp (°F)
Tank Outlet water temp (°F)
Mixing valve (F) Outlet temp (°F)
Flow meter (Total gallons)
Flow meter (tank gallons)
Tank heat elements (kW)
Inlet mains temp (°F)

4. Solar Flat Plate System with photovoltaic (PV) DC pump with 80-gallon storage

This system is identical to the solar reference system described in #2 above. The AET DPV-80-40 is composed of an AE-40 Collector (4' x 10'), American Water Heater Co. Model OST-80TCE Storage Tank (80-gallon) but features a Laing D5 pump w/10W Power-Up Module. The solar tank has a single 4500-watt auxiliary heating element. The thermostat and mixing valve were set to 120°F.

Measurements for System 4
Inlet water temp (F)
Tank Outlet water temp (F)
Mixing valve Outlet temp (F)
Solar collector Send (F)
Solar collector Return (F)
Flow meter Total (gal.)
Flow meter tank (gal.)
Tank Electric Element (kW)

5. Gas Water Heater – Standard Residential 40-gallon

The 40-gallon standard residential GE GG40T06AVG has a rating of 36 KBTU/hr., with a first hour rating of 67 GPH. Tank dimensions are 61.75 in. (H), and 17.7 in. (dia.).

Measurements for System 5
Inlet water temp (°F)
Outlet water temp. (F)
Flow meter (gal.)
Gas meter (cu. ft.)

6. Tankless Gas Heater

The Takagi TK-3 natural gas heater has a maximum energy rating of 199K Btuø. It also utilizes 120V to power its on-board electronic controller. The unit requires 0.4 GPM for continuous fire after initial ignition.

Measurements for System 6
Inlet water temp (°F)
Outlet water temp. (°F)
Flow meter (gal.)
Gas meter (cu. ft.)
Parasitic power (W)

7. Tankless Electric Heater

Seisco RA-22, 240 VAC Power: 22kW Max., 91 Amps (max.), 4 x 5500W heating elements (one gallon), EF = 0.99, 2.3 gpm at 65°F rise (138.7 gph).

Measurements for System 7
Inlet water temp (°F)
Outlet water temp. (°F)
Flow meter (gal.)
Total Power (kW)

Testing of 10 W Photovoltaic Module

The Power-Up 10 Watt module (BSP 1012) used in the flat plate solar thermal system was submitted to testing in our flash simulator with the purpose of characterizing its I-V curve prior to installation. The module was tested in September 2008, and the results can be observed in Figure 5.

Table 3 lists the specific parameters measured under testing (Isc, Imp, Voc, Vmp and Pmp) and compares to those on the back plate label provided by the manufacturer.

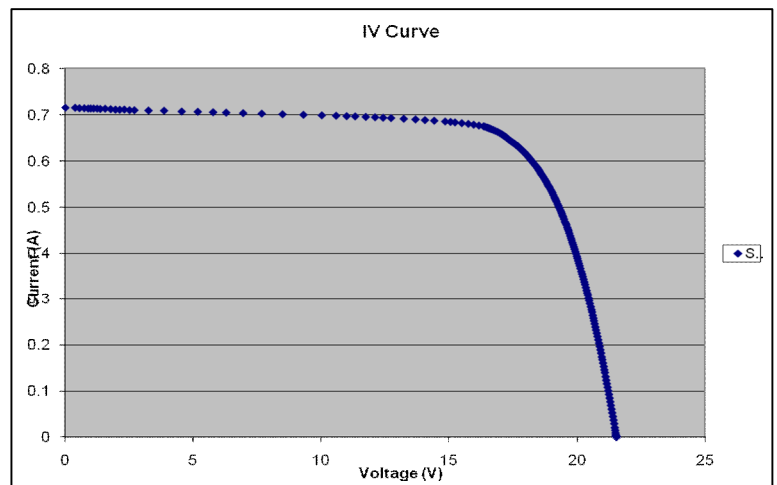


Figure 5. Current and voltage (I-V) curve of the power up 10 watt under FSEC flash simulator testing at standard conditions 6 STC. (Testing courtesy of Kris Davis, FSEC).

Table 3
Voltage and Current Parameters of Power Up 10 Watt Module Compared

Power-Up BSP 1012	Flash Simulator Measurements	Label on back Plate
Isc (A) at STC	0.71	0.66
Imp (A) at STC	0.65	0.58
Voc (V) at STC	21.52	21.3
Vmp (V) at STC	17.24	17.3
Pmp (W) at STC	11.20	10.03

Test Protocols and Established Draws

During the summer of 2008, the Building America (BA) team worked to determine a suitable hot water draw pattern for testing. In consultation with the National Renewable Energy Laboratory (NREL), a decision was made to alternate between ASHRAE 90.2 and a draw schedule that better represents typical family hot water usage. A new hot water draw schedule was created based on previously described procedures (Hendron and Burch, 2007), which we refer to as the NREL/BA draw profile.

The hot water draw profile was developed from BA source documentation with the addition of hot water loads changing on a monthly basis. The decision to adjust the quantity of daily hot water draws on a monthly basis was due to the degree of mains inlet temperature variations observed in central Florida throughout the year including empirical data as detailed below.

Seasonality of Water Heating Loads: Inlet Water Temperature Variation

Although water heating is not completely dominated by weather as with space heating and cooling, its loads are still very sensitive to inlet water temperature conditions which, in turn, are very sensitive to ambient air temperatures. Although source water may come from either surface or deep wells, the transmission pipes travel long distances in the ground at relatively shallow depths.

Figure 6 shows how daily average hot water energy use varied with the daily average air temperature in a sample of 150 electric resistance hot water heaters monitored over a full year (Masiello and Parker, 2002). Although there is scatter in the plot, a simple linear regression plotted shows that daily outdoor air temperature justifies 82% of the variation in the day-to-day hot water energy consumption. Moreover, the same graph suggests that daily energy for heating hot water varies by fully 2:1.

Table 4
NREL/BA Monthly Gallons Draw Variations

Month	Hot Water Gallons Per Day	
January	67.2	Highest daily draw
February	66.4	
March	66.4	
April	63.8	
May	54.6	
June	48.4	
July	42.2	Smallest daily draw
August	44.0	
September	44.9	
October	47.5	
November	53.7	
December	59.0	
Average	54.84	

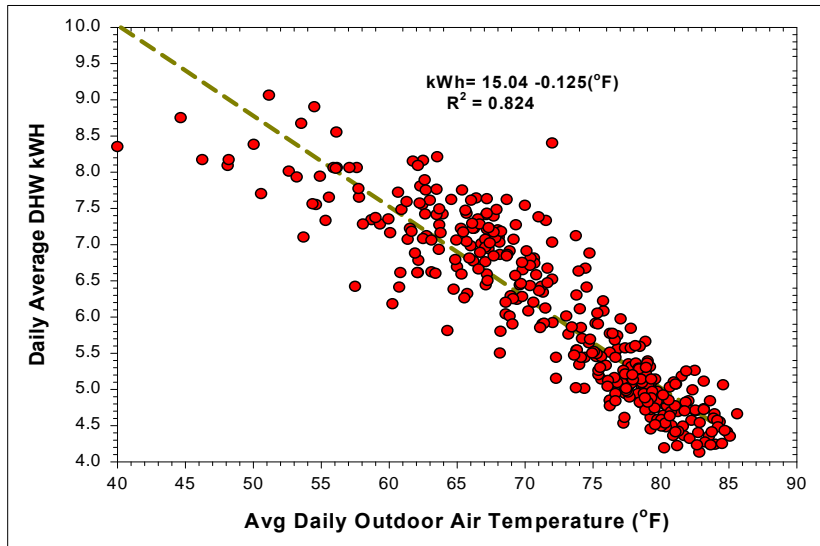


Figure 6. Impact of air temperature on daily DHW use.

Figure 7 shows the same data summarized by month with the bi-modal daily water heater electrical load shape plotted over a 24-hour cycle. Here, we can clearly see a substantially lower level of water heating load in summer versus winter. The water heating loads are greatest during the colder months. April clearly shows the shift in timing of water heating load imposed by Daylight Savings Time. The later spring and summer months show progressively lower water heating loads. Even evaluated on a monthly basis, which masks temperature extremes, water heater daily energy varies by 63% from January to July.

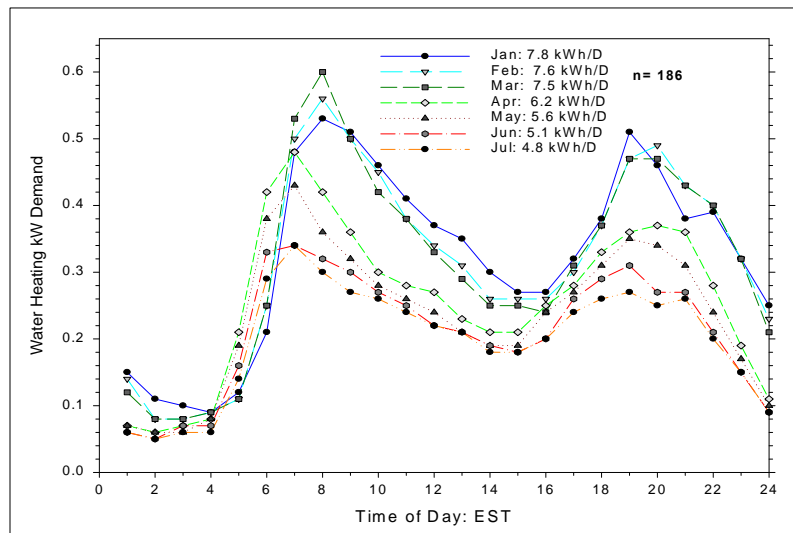


Figure 7. Measured DHW load profiles by month.

There are several reasons for this influence; however the most important source of variation comes from the variation of the inlet water temperature itself. As measured at the HWS lab, inlet tap water temperatures vary seasonally by about 34°F in Central Florida as seen in Figure 8. Although the annual inlet water temperature averages 75.4°F, it varies to a high of about 85°F from June thru August to a low of 51°F in December since ground water piping is affected by weather conditions.

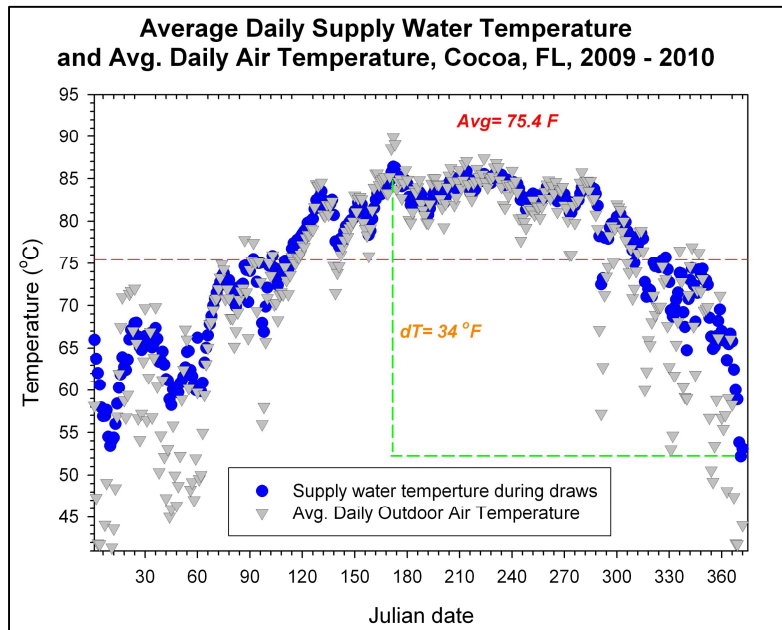


Figure 8. Variation of mains water temperature over the year in central Florida.

Importance of Inlet Water Temperatures

Given that water is commonly heated to 120°F, 50 gallons heated from 86°F on the hottest summer day would require 4.15 kWh without any standby losses. However, 50 gallons heated from 51°F would require 8.4 kWh of heat without standby losses on the coldest winter day ó a 2:1 difference (4.3 kWh difference) in the magnitude of water heater energy loads from summer to winter peak and almost exactly mirroring the variation seen in measured consumption from summer to winter in Figures 6 and 7.

It is noteworthy that this effect is not confined to Florida. Data collected in the Pacific Northwest by Pratt et al., 1989 showed that the measured electricity use of 220 resistance water heaters there varied from 9.8 kWh per day in August to 14.4 kWh in January ó (4.6 kWh/day) or a 47%.

Seasonal Variation in Florida Hot Water Use

As noted earlier, the variation in the inlet water temperature in Central Florida not only creates differences in the energy needed to raise water temperature to 120°F, but it also leads to a changing volume of hot water used in residences. This phenomenon is important for understanding how to properly simulate hot water loads in a realistic sense throughout the year.

A seasonally changing water volume is seen because for hot water end-uses, such as bathing and washing hands, occupants prefer a mix temperature of 100 to 105°F. Conversely, the hot water uses for machine-related draws (washing machines and dishwashers) are generally unaffected by this outcome. Still, the hot water used for showers, baths and hand washing is significant ó resulting in 70% or more of total hot water use. Since hot water storage or supply temperatures are often about 120°F, the amount of cold mixed to achieve 100°F at the shower outlet varies strongly with inlet cold water temperature.

As illustrated in Figure 8, the inlet water temperature in Central Florida varies from a low of about 51°F in December thru January to a high of 85°F in July thru August. This 34-degree inlet temperature difference has a large impact on the hot to cold water mix volume. Thus, to achieve a 105°F shower in January would require a 78% mix of hot and 22% cold. Consequently, a one gpm shower would need 0.78 gpm of hot in winter to keep the bather thermally comfortable. However, in August, where the inlet water temperature is 85°F, the required hot water is much less: 58% hot to 42% cold. Hence, the volume of hot water to achieve 105°F shower in August would be only 0.58 gpm hot ó 26% less hot water than in January. Since temperature sensitive draws likely account for about 70% of hot water use (Lowenstein and Hiller, 1996; DeOreo and Mayer, 2000), we would expect that hot water consumption would vary in volume in Central Florida by about 18%. Finally, it was recently documented that people in the colder part of the year prefer up to 4°F hotter bathing temperatures (Ohno et al., 2000). This fact would further accentuate the previously observed variation.

Greater seasonal draws in winter have been verified in two separate monitoring studies at FSEC. One study was completed by Merrigan (1983) on 17 electric resistance water heaters in Florida where the volume of hot water was measured. This study, with the results reproduced in Figure 9, showed hot water consumption varying from a low of 47 gallons per day all the way up to 74 gallons per day in January with an average use of 60 gallons per day. As a result, monthly consumption varied by about 35% from highest to lowest. The data are shown in Figure 10.

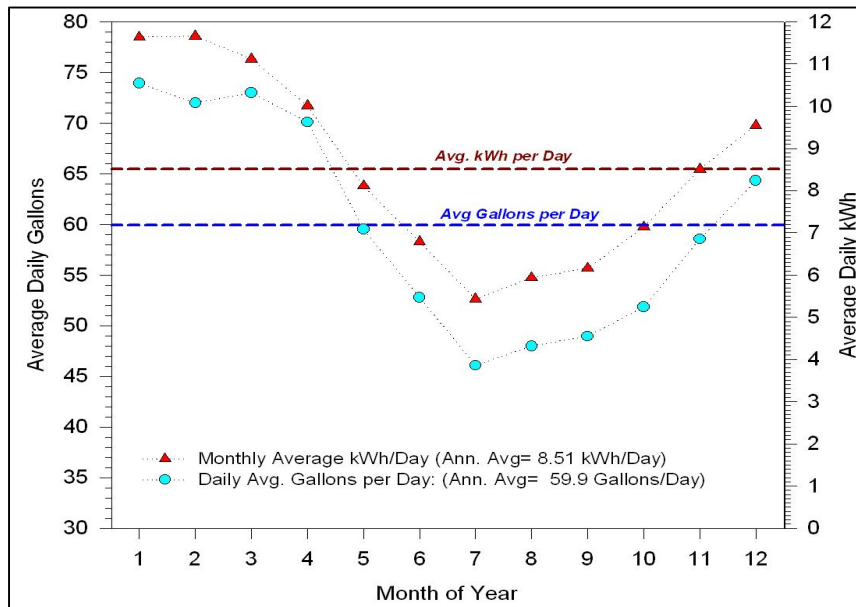


Figure 9. Variation in monthly daily average hot water consumption in 17 measured electric water heating systems.

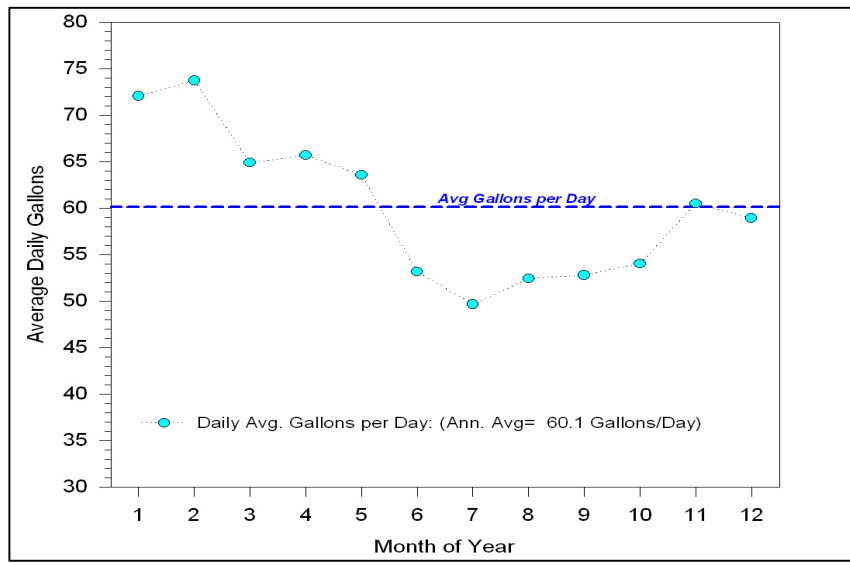


Figure 10. Measured monthly variation in hot water consumption in 35 electric water heaters in Florida (1997).

Another study was completed for the Solar Water Heating Applications Program (SWAP) (Long and Harrison, 1998). Here the average measured hot water gallons per day by month in 1997 for all 35 SWAP sites averaged about 60 gallons per day (occupancy was uncharacteristically high in the low-income homes) but varied from a high of about 74 gallons in February to a low of about 50 gallons: a range in monthly consumption of 32%. Thus, consumption in January thru February is about 20% greater than the average while consumption in July is about 15% lower.

To realistically account for this effect in the BA/NREL profile, we adjusted the volume of hot water drawn each month by the monthly variations seen in the Merrigan study. This modification resulted in the following multipliers for the absolute quantity of hot water in the BA/NREL profile:

Table 5
Monthly Volume Multiplies for BA/NREL Profile

Month	Multiplier
1	1.2320
2	1.2167
3	1.2167
4	1.1683
5	0.9920
6	0.8800
7	0.7680
8	0.8000
9	0.8160
10	0.8640
11	0.9760
12	1.0720

The amount of hot water gallons drawn per month under a NREL/BA draw profile are listed in Table 4. The NREL/BA draw profile was officially implemented for testing at the HWS Lab during the latter part of May 2009. Rotations between the two draw schedules were carried every two weeks for each month.

Figure 11 shows the differences by hour between the ASHRAE 90.2 and the NREL/BA draw profiles. The NREL/BA draw schedule represents a realistic family draw pattern as opposed to the hourly events adopted in ASHRAE 90.2. Unlike the NREL/BA draw profile, the ASHRAE draws remain constant at 64.3 gallons per day throughout the year.

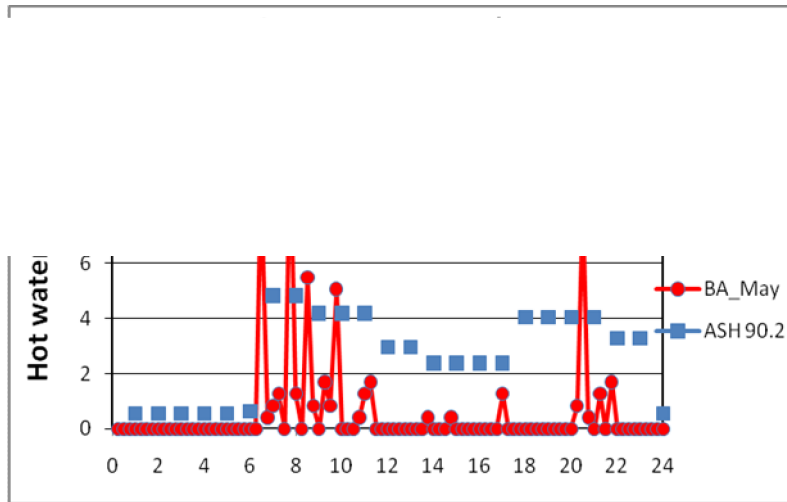


Figure 11. Comparison of ASHRAE 90.2 and NREL/BA (May) draw profiles

Hot Water Supply Temperature

During late February 2009, all water heating systems were set to deliver a target output temperature of 120°F. In fact, the combined hot water temperature delivered by all systems through mid-November 2009 averaged 119.8°F (from Table 6). However, to control higher temperatures and scald danger generated by the solar systems, a mixing valve was utilized on the three systems to limit hot water temperatures to the desired target.

Generally, lower averaged values of outlet hot water temperature were obtained from the tankless systems. This occurrence is due to the lag associated with startup firing exhibited by the tankless designs (Figure 12). As a result, the tankless gas system was set to 122°F via its own electronic controls while the tankless electric was set in increments until the delivery temperature averaged the desired

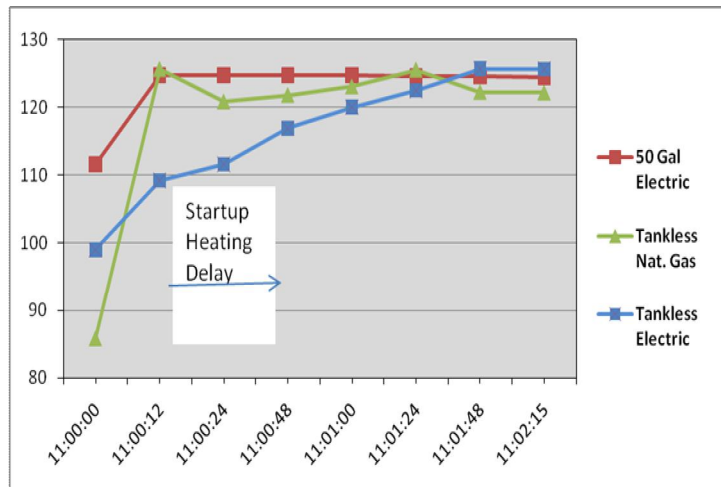


Figure 12. Delivery temperature lag seen in tankless water heaters upon startup.

test setting. During January 2009, hot water output delivery was observed to compare the startup delivery temperature of the reference standard electric tank against the tankless heaters.

Twelve second sample data taken during a routine morning draw (11:00 AM) was plotted (Figure 13) and can be observed from its initial startup (standby) until it is stabilized. Data suggests that longer delays at startup by a system to heat water to 120°F under demand can contribute to wasted energy and water resources.

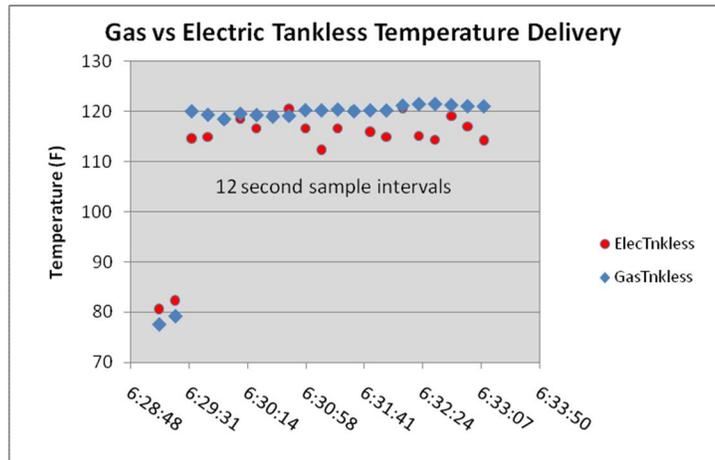


Figure 13. Comparative stability of storage vs. tankless system delivery temperature.

Tankless Electric System

In June 2009, the manufacturer replaced the tankless electric unit with a current production model. This unit performed better at startup indicating that the manufacturer has addressed the issue. However, other issues with the thermostat set point are beginning to re-appear at the end of the analysis period, such as a slight decline in averaged delivery temperatures from 116.0°F delivered in June to 115.7°F in November. The new unit also showed a higher degree of temperature variation during operation.

Using infrared thermography, we also noted that the tankless electric system has substantial heat losses through the heat transfer jacket during operation (Figure 14). These losses were found to adversely impact the performance of the system such that its advantage over the conventional storage electric system is not pronounced, particularly when shed temperatures are lower. Thus, while the system has no standby losses when hot water is not being used, it does have thermal losses during operation.



Figure 14. IR and visible images of heat loss from tankless electric water heater in operation.

Experimental Log

An experimental log was created to document key events over the months of testing. The log link is also visible and available for viewing on the infomonitors.com/HWS website. The majority of entry logs are related to dates when draw profile schedules were being changed. This feature allows easy reference to determining dates for analyses. The on-line log also documents any problems that have surfaced with monitoring equipment or mechanical failure during testing. The majority of mechanical problems were observed between September and October. Below is a summary of entries related to events that prevented continuity of testing.

- *6/26/09 Natural gas 40 gal. system down 6/25 for water inlet distribution manifold leak repair. Schedule on all other systems disrupted 6/26 between 9:30 and 12:30 PM. Operation restored on NG 40 gallon tank at 3:30 pm.*
- *9/30/09 Problem with flowmeter in morning hours draw schedule preventing log of BTU's, resulting in lower daily efficiency.*
- *10/05/09 Flowmeter replaced on ICs/50 Gal. system due to failure. Previous two days (weekend) No BTU data.*
- *10/14 - 10/14/09 Natural Gas tank meter went thru a series of fixes. Good known data leading to $Eff=0.56$ begins on Oct. 15, 2009*
- *10/19/09 Replaced freeze valve on Diff. Solar system*
- *10/20 - 10/22/09 Flat plate PV system down, check valve removed and cleaned, air shred valve adjusted, solenoid valve replaced. Last good $Eff = 1.8$ on Sat. 10/17.*

The flawed data in the data stream were removed prior to analysis.

Analysis and Results

Evaluation of Impact of Pipe Insulation During Shakedown

Between March 3rd and 10th, 2009 FSEC staff applied foam insulation (R-2) to all piping located inside the HWS building. An evaluation of the impact of piping insulation was performed for similar matched data prior to and after insulation ó four matched periods with similar conditions. While we found that the measured performance at the water heater outlet did not vary much with pipe insulation, we found a dramatic impact on the two solar systems which circulated during the day. A summary of the fundamental findings shows:

- The average daily operating COP of the flat plate differential system increased from 5.54 to 8.30 by the insulation, corresponding to an increase in solar fraction relative to the reference electric resistance system of 83.8% to 89.3%.
- The average daily operating COP of the flat plate PV pumped system increased from 3.69 to 6.06, corresponding to an increase in solar fraction relative to the reference electric resistance system of 75.6% to 85.3%.
- The average daily operating COP of the ICS system increased from 1.86 to 2.12, with an increase in solar fraction relative to the electric resistance system of 51.5% to 58.4%.

Hence, the data shows during February/March conditions that pipe insulation exerts between a 5 and 10% influence on achieved solar fraction ó highly significant given its low cost. It should also be noted that the exterior pipe sections were already insulated for the solar systems, and this influence is solely from insulating the segment of the piping inside the test lab interior. We further conclude that improvements to pipe insulation technology could provide significant improvements to solar system performance, particularly under winter conditions.

Summary of Results

Between the period of March 11, 2009 and February 28, 2010, the overall combined efficiency using both ASHRAE 90.2 and NREL/BA draw patterns was plotted (see Figure 15). Monthly data are summarized in Table 6. Parasitic energy is included in the calculations for those systems that have auxiliary energy requirements, such as controllers in the natural gas tankless and differential activated pump in the solar system. Unsurprisingly, results from testing indicate that daily efficiency for these systems is somewhat below the published energy factor ratings.

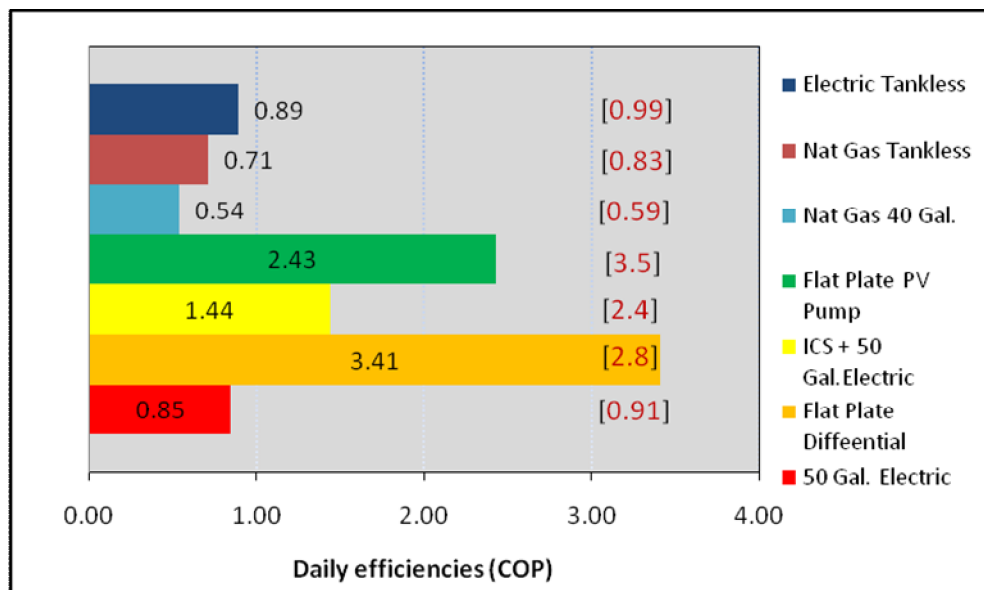


Figure 15. Comparative average COP of tested systems over eight month period.

A primary reason for these results is that the reduced amount of hot water utilized since May 2009 when using the NREL/BA schedule yields lower efficiencies, particularly on standard electric and gas systems when compared to the ASHRAE 90.2 (draws 64.3 gpd). As expected, the solar flat plate systems display the highest average daily efficiency for the 12-month period (COP of 3.63 and 2.70). Although the PV-pumped solar flat plate demonstrated the highest efficiencies during the first six months, it is evident that performance begins to diminish in November 2009. Further decline in performance was observed during reduced solar radiation periods. For example on December 2009, integrated solar radiation was limited to 2,623W/m². The solar flat plate differential AC and PV-pumped systems demonstrated daily COP efficiencies of 2.26 and 1.10 respectively. In summary, it is evident that during cloudy days the differential controlled flat plate solar system performs better than the PV-pumped system. Data for those days also suggest that a large photovoltaic module might improve efficiency for the passive solar system during mild or cloudy weather.

Table 6A
Monthly Performance at HWS Facility . 2009

	Feb. 2009	Mar. 2009	April 2009	May 2009	June 2009	July 2009	August 2009
Electricity Usage– kWh/day							
Electric Tank	9.18	8.80	8.01	6.48	5.80	5.81	5.62
80 Gal Diff Flat Plate	2.57	1.95	1.44	1.35	0.88	1.01	0.74
ICS w/50 Gal Electric	5.75	4.65	3.76	3.13	2.31	2.72	2.01
80 Gal PV Pump Flat Plate	3.43	2.13	1.42	0.98	0.22	0.39	0.04
Tankless Electric	8.63	8.97	8.80	7.65	4.90	4.86	4.75
Natural Gas Usage – therms/day							
50 Gal Nat Gas Heater	0.472	0.510	0.431	0.331	0.277	0.244	0.181*
Nat Gas Tankless Heater	0.317	0.428	0.287	0.236	0.224	0.219	0.216
Weather Conditions							
Solar (W/m ²)	181.4	211.0	241.0	241.0	247.0	250.0	229.0
Outdoor Temp	61.0	67.7	72.2	79.4	83.6	83.1	84.8
Shed Temp	69.0	74.2	78.5	84.1	88.0	87.2	89.0
Daily Efficiencies COP							
Electric Tank 50 Gal	0.89	0.90	0.88	0.86	0.85	0.81	0.82
80 Gal Diff Flat Plate	3.39	4.27	5.20	4.70	6.57	5.51	7.92
ICS W/50 Gal Electric	1.55	1.82	2.01	1.99	2.37	1.96	2.62
80-Gal PV Pump Flat Plate	2.48	3.92	5.54	6.66	26.61	13.55	133.24
40 Gal Nat Gas Tank	0.55	0.54	0.54	0.54	0.54	0.65	0.80*
Tankless Nat Gas	0.80	0.76	0.77	0.77	0.75	0.73	0.71
Tankless Electric	0.89	0.89	0.89	0.89	0.92	0.90	0.91
Total Daily Gallons – gals/day							
Electric Tank 50 Gal	59.1	64.0	63.5	57.6	53.2	51.7	53.1
80 Gal Diff Flat Plate	59.0	63.3	62.8	56.9	53.0	51.6	52.9
ICS W/50 Gal Electric	59.6	63.4	62.4	56.8	52.8	51.8	52.1
80-Gal PV Pump Flat Plate	59.6	63.0	63.1	57.5	53.7	52.0	53.2
40 Gal Nat Gas Tank	59.5	64.2	63.8	57.7	51.7	54.9	55.5
Tankless Nat Gas	59.8	62.9	64.5	59.4	56.9	55.2	55.7
Tankless Electric	59.4	63.7	63.0	56.7	53.2	51.8	53.5
Draw-Weighted Inlet Temps							
Electric Tank 50 Gal	64.8	71.9	75.4	80.5	82.4	82.8	84.2
80 Gal Diff Flat Plate	64.9	71.9	75.4	80.4	82.3	82.8	84.1
ICS W/50 Gal Electric	96.4	103.9	108.3	109.9	112.6	109.1	114.6
80-Gal PV Pump Flat Plate	64.7	71.5	75.2	80.2	82.0	82.5	83.7
40 Gal Nat Gas Tank	64.1	71.7	75.4	80.7	82.4	83.0	84.3
Tankless Nat Gas	64.8	71.9	75.	80.4	82.4	82.8	84.1
Tankless Electric	64.7	71.7	75.3	80.0	81.8	82.4	83.7
Draw-Weighted Outlet Temps							
Electric Tank 50 Gal	121.3	119.5	121.0	120.1	120.2	119.9	119.4
80 Gal Diff Flat Plate	119.2	119.1	120.6	121.1	122.5	121.5	123.1
ICS W/50 Gal Electric	121.5	119.9	121.7	121.2	120.9	120.5	120.7
80-Gal PV Pump Flat Plate	120..8	121.0	124.3	124.4	124.4	122.4	125.9
40 Gal Nat Gas Tank	117.4	119.1	120.3	118.0	117.6	117.8	116.2
Tankless Nat Gas	116.4	117.7	117.5	117.8	118.3	118.2	118.1
Tankless Electric	117.5	117.5	126.2	128.8	116.2	116.7	116.5

Table 6B
Monthly Performance at HWS Facility . 2009

	Sept. 2009	Oct. 2009	Nov. 2009	Dec. 2009	Jan. 2010	Feb. 2010	Mar. 2010	Annual
Electricity Usage– kWh/day								
Electric Tank	5.65	5.94	7.16	8.51	10.52	10.41	9.75	2692
80 Gal Diff Flat Plate	1.08	1.44	2.23	3.51	4.36	4.27	3.41	635
ICS w/50 Gal Electric	2.60	3.03	5.48	7.96	9.29	9.39	7.47	1703
80 Gal PV Pump Flat Plate	0.57	2.13	2.75	5.86	8.13	7.18	5.05	959
Tankless Electric	4.87	5.16	6.25	8.03	10.12	10.2	9.60	2556
Natural Gas Usage – therms/day								
50 Gal Nat Gas Heater	0.225*	0.289	0.417	0.501	0.619	0.615	0.569	140.1
Nat Gas Tankless Heater	0.225	0.233	0.280	0.340	0.393	0.407	0.407	105.9
Weather Conditions								
Solar (W/m ²)	199.1	176.3	169.0	134.0	192.7	194.9	232.0	177.5
Outdoor Temp	81.8	78.8	69.6	64.5	55.0	55.5	61.8	73.1
Shed Temp	86.6	84.3	75.8	71.0	62.6	63.2	68.5	78.8
Daily Efficiencies COP								
Electric Tank 50 Gal	0.82	0.82	0.85	0.86	0.87	0.87	0.87	0.86
80 Gal Diff Flat Plate	5.29	4.28	2.96	2.52	2.57	2.63	2.89	3.63
ICS W/50 Gal Electric	1.71	1.61	1.28	1.07	1.16	1.15	1.33	1.51
80-Gal PV Pump Flat Plate	9.35	2.52	2.36	1.42	1.23	1.44	1.89	2.70
40 Gal Nat Gas Tank	0.69*	0.58	0.51	0.52	0.54	0.54	0.54	0.56
Tankless Nat Gas	0.69	0.69	0.70	0.72	0.76	0.74	0.70	0.73
Tankless Electric	0.89	0.88	0.88	0.88	0.89	0.89	0.90	0.89
Total Daily Gallons – gals/day								
Electric Tank 50 Gal	50.9	51.3	55.4	59.2	63.7	63.9	62.8	57.3
80 Gal Diff Flat Plate	50.2	50.2	54.4	58.6	63.3	64.5	63.2	56.8
ICS W/50 Gal Electric	50.2	50.4	54.8	59.1	62.3	65.5	64.4	57.0
80-Gal PV Pump Flat Plate	50.8	50.7	55.1	59.2	62.6	64.8	63.3	57.1
40 Gal Nat Gas Tank	53.6	51.2	59.5	62.2	66.7	67.4	66.4	59.3
Tankless Nat Gas	53.5	50.8	58.2	62.9	67.5	68.2	67.3	59.9
Tankless Electric	51.7	52.2	55.8	60.8	65.6	66.7	65.8	57.8
Draw-Weighted Inlet Temps								
Electric Tank 50 Gal	82.4	80.7	75.1	69.7	61.9	62.6	65.1	75.3
80 Gal Diff Flat Plate	82.4	80.7	75.2	69.8	62.0	62.7	65.1	75.3
ICS W/50 Gal Electric	110.3	107.9	94.5	82.8	80.9	80.4	89.3	100.6
80-Gal PV Pump Flat Plate	82.0	80.3	75.1	69.6	62.2	62.7	64.9	75.1
40 Gal Nat Gas Tank	82.3	80.5	74.9	69.4	61.6	62.3	64.8	75.2
Tankless Nat Gas	82.4	80.6	75.3	69.8	62.1	62.7	65.1	75.3
Tankless Electric	81.9	80.2	75.0	69.5	61.9	62.4	64.9	75.0
Draw-Weighted Outlet Temps								
Electric Tank 50 Gal	119.4	119.3	120.0	120.0	120.4	120.2	120.3	120.0
80 Gal Diff Flat Plate	120.6	120.6	119.2	119.9	120.1	120.3	119.7	120.7
ICS W/50 Gal Electric	120.4	120.4	120.6	121.1	121.8	121.8	121.5	120.9
80-Gal PV Pump Flat Plate	122.3	120.6	118.4	120.6	120.0	121.2	121.5	122.1
40 Gal Nat Gas Tank	117.7	118.0	118.7	120.1	122.9	122.8	121.4	119.2
Tankless Nat Gas	118.2	117.0	116.6	117.6	117.0	117.2	117.4	117.6
Tankless Electric	116.1	115.8	115.1	117.1	117.8	117.9	118.2	118.6

Daily Electric Consumption

A comparison of daily electric consumption for five systems is illustrated in Figure 16 and Table 6. The baseline electric resistance system shows an average energy use of 6.5 kWh per day or about 2,372 kWh if it extrapolated to an annual basis. This result compares favorably with measured average energy use of 2,240 kWh/year in a field test on 150 sub-metered electric resistance storage water heaters systems in Central Florida (Masiello and Parker, 2005).

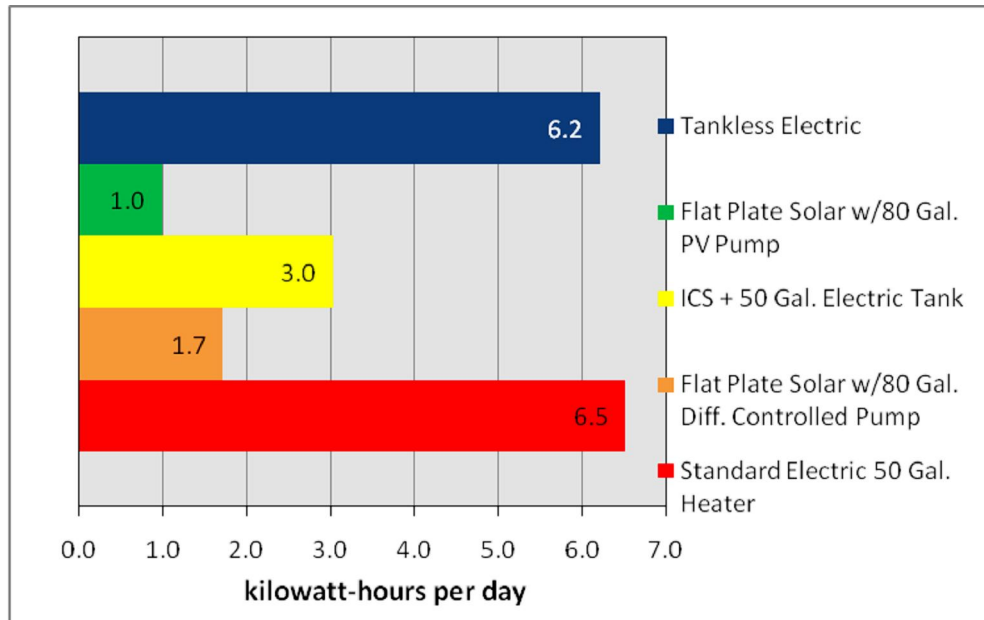


Figure 16. Daily average electricity use for water heating.

The data indicates a small 0.3 kWh daily reduction for the tankless electric when compared to the standard electric baseline system. Solar systems clearly demonstrate large daily electric reductions of between 5.5 and 3.5 kWh per day.

Time of day Electric Demand

Electric demand for five systems was also analyzed for the period between March and February 2010 to determine impact on time-of-day-peak loads and load shape (Figure 17). The plot reveals a dramatic peak load reduction of flat plate solar systems when compared to the standard baseline electric ó particularly during the critical utility 7 to 8 AM hour.

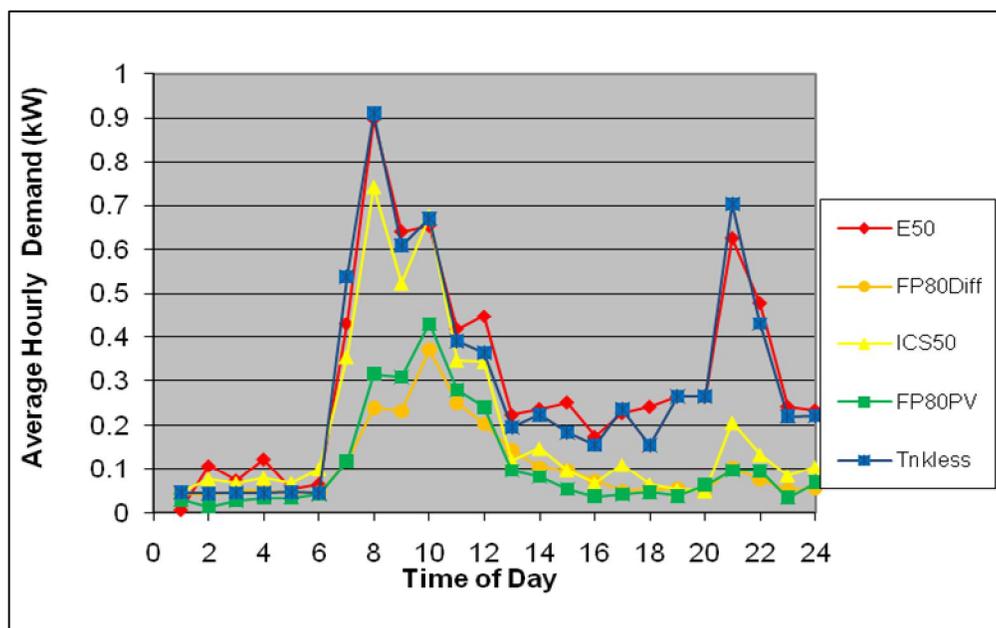


Figure 17. Impact of water heating systems on electrical load shape over eight month period.

When evaluated on an annual basis, morning peak demand reduction by the two solar flat plate systems appears to be reduced on average by 86%. Furthermore, the flat plate solar systems appear to have shifted the daily peak two hours after that experienced by the electric resistance system (10:00 AM). Peak demand reduction for the ICS solar systems is lower by 35%. Demand for all solar thermal systems in the afternoon appears flat and limited to 0.2 kWh. During typical afternoon peak periods the active solar systems were at 0.05 kW and the ICS at or below 0.1 kW while the tank and tankless electric created 0.25 kW demand.

The highest average peak demand throughout the study was observed during the NREL/BA hot water draw events in February 2010 (Figure 18). The morning peak is again observed at 8:00AM for the standard 50-gallon electric system. The flat plate and ICS solar systems managed to reduce peak by 73% and 30% respectively; however the tankless electric shows signs of a peak incremental increase of 11% in the morning and 61% in late hours of the night (9:00 PM) even when aggregated over a one hour period. The ICS manages to reduce the evening peak by 50% at night.

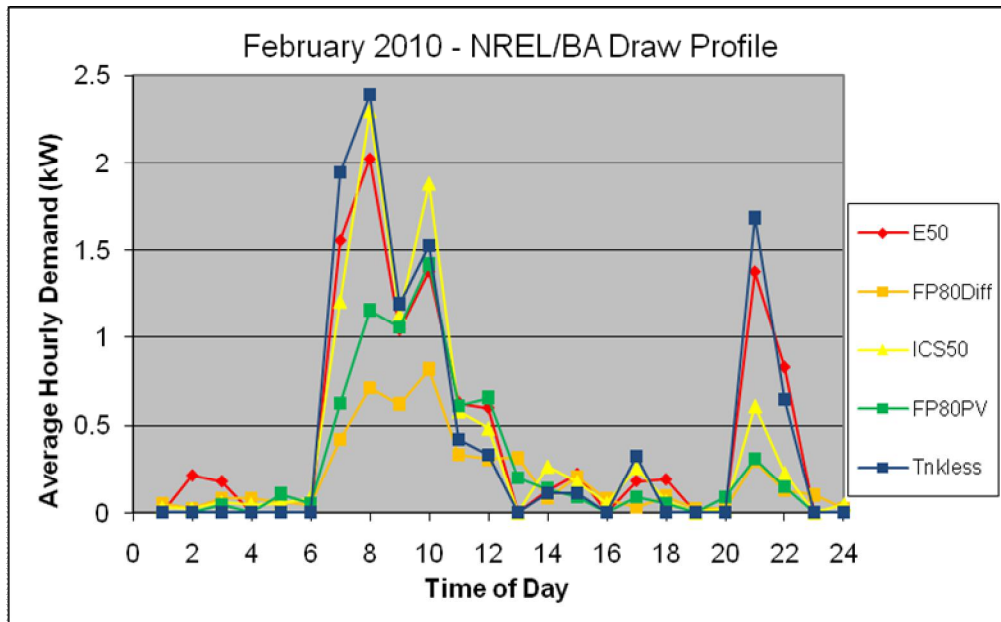


Figure 18. Impact of water heating systems on electrical load shape obtained by using NREL/BA draw profile.

It must be emphasized that these peak impacts will be influenced by the time period chosen for the data aggregation. Thus, the impacts of the tankless electric system may be greater when the data is averaged on a 5-minute or 1-minute basis.

Summer and Winter Peak Day Analysis

Information relayed to FSEC as experienced by Florida's largest investor owned utility (IOU), FPL on peak day, revealed the following time of day and peak power generation.

Table 7
2010 Utility Coincident Peak Periods

	Year	Date	Time of day	Generated Power
Summer Peak	2009	6/22/09	4-5 PM	22,351 MW
Winter Peak	2010	1/11/10	7-8 AM	24,346 MW

Summer peak occurred during June 22, 2009 at 5:00 PM (which is 4:00 PM with our standard time used in our database). The table also indicates that the utility peak coincident winter day was January 11, 2010 with the peak occurring at 8:00 AM. Evaluation from these hot water systems on peak days follows:

Summer Peak Hour (June 22, 2009, 5:00 PM)

For the electric systems, the peak values were zero during the late afternoon except for the differential pumped system: 0.074 kW and the tankless electric 0.038 kW which represent the respective demand utility summer peak coincident reductions. During this day, the hot water draw pattern used at the time was the NREL/BA schedule.

Winter Peak Hour (January 11, 2010, 8:00 AM)

During this day, the hot water draw pattern used at the time was the ASHRAE 90.2 schedule.

Standard System (resistance electric): 0.852 kW

Differential Solar System: 0.409 kW (with pump energy)

ICS + 50 Gal. electric system: 0.746 kW

PV pumped solar system: 0.838 kW (** System not operating, caused by solenoid valve failure)

Tankless Electric: 0.849 kW

Demand reduction, as compared against the standard baseline system (electric resistance E50) during winter peak day, can be observed in Figure 19. The differentially pumped flat plate solar system (FP80 Diff) showed a substantial 52% peak reduction. Peak reduction for the ICS50 system shows a steady reduction in the afternoon but a less favorable decrease during morning hours. During winter peak day, data reveals that outdoor temperatures reached 29.3°F at 7:00 AM (15-minute average). Temperatures inside the HWS Laboratory registered an average low of 37.6°F at 7:00 AM.

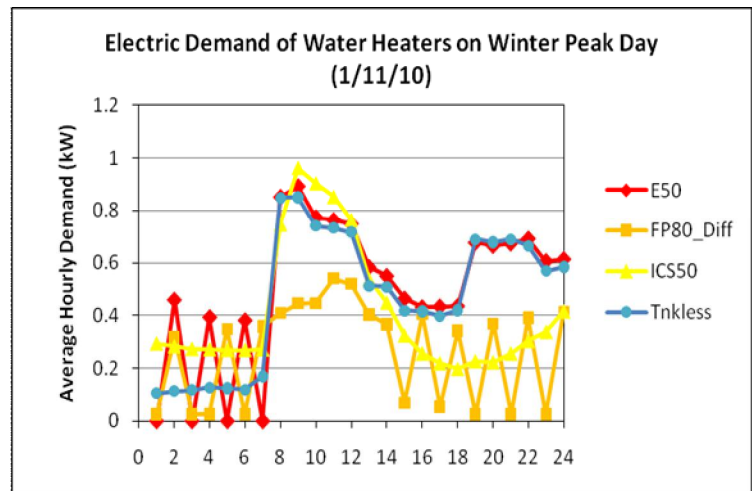


Figure 19. Winter peak utility coincident demand

Impact of Raw Profile and on Seasonal Efficiency

Reference Standard Electric 50 Gallon Tank

Further analysis was performed on the two draw profiles to characterize monthly efficiency and time of day demand for all systems. Figure 20 presents the effects on electrical efficiency (COP) demonstrated by the reference standard electric system. Results from two draw schedules are shown due to the distinctive hot water draw patterns. A large overall decrease in efficiency is observed with the NREL/BA pattern, as it utilizes less hot water during the summer months. In addition, the magnitude of standby losses increase relative to delivered hot water energy.

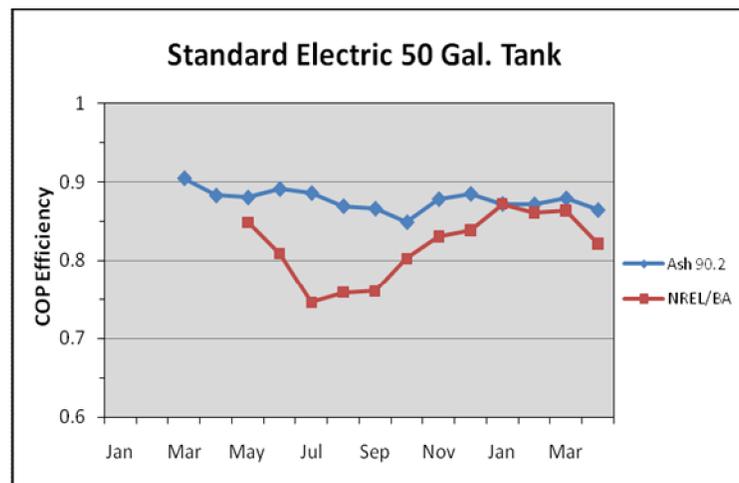


Figure 20. Efficiencies by month for the reference standard electric water heater under ASHRAE 90.2 and NREL/BA draw patterns.

As illustrated in Figure 21, warmer inlet temperature from mains water supply are evident during the summer months of 2009, leading to decreased measured energy output delivery during draws.

Tankless Electric

In a similar way, Figure 22 shows the efficiencies for the tankless electric system measured from both hot water draw patterns.²

During the month of June, an increase in efficiency was noted after unit replacement. However, a small but steady decrease in efficiency was recorded under the ASHRAE 90.2 draw schedule between August 2009 and February 2010. Furthermore, a marked decrease in efficiency was noticed with NREL/BA draws following initial installation during June. Infrared thermograph (see Figure 12) shows that contrary to expectations, the tankless electric system has large thermal losses through its outer jacket during operation. This lower efficiency is particularly during shorter draws and is caused by residual heat that is dissipated and lost.

Natural Gas 40 Gallon Storage Tank

Figure 23 presents the efficiencies measured for the standard natural gas hot water heater (40 gallons) since March 2009. It is important to mention that the natural gas meter pulser mechanism experienced alignment failure. Data suggested that efficiencies between July and August 2009 were too high. Consequently, these errant data were not included in the analysis. To address this problem, efficiencies for those months are

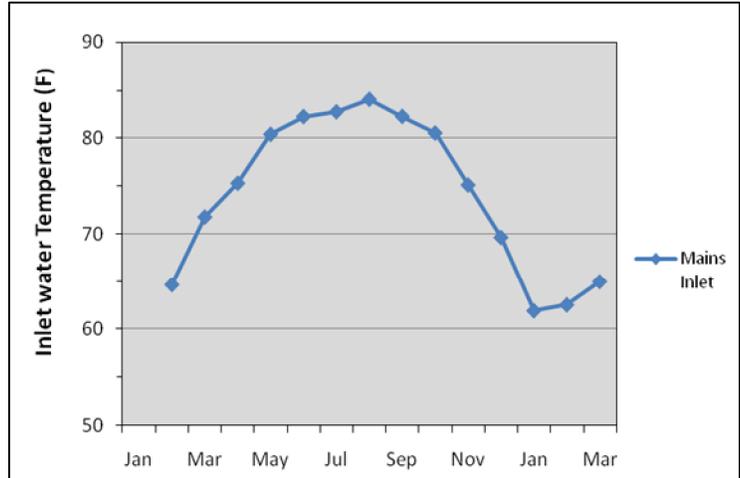


Figure 21. Monthly variation in inlet water temperature.

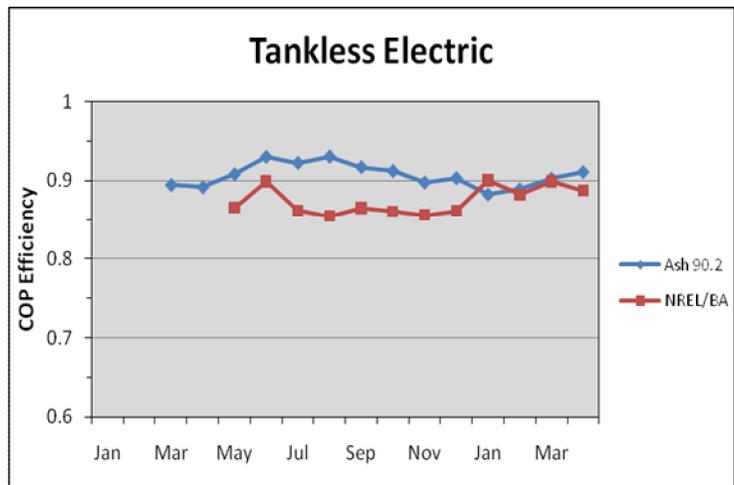


Figure 22. Efficiencies by month for the tankless electric water heater under ASHRAE 90.2 and NREL/BA draw patterns.

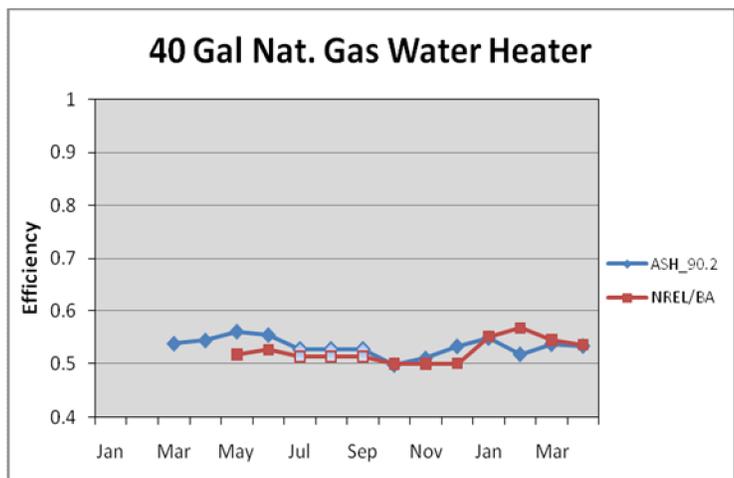


Figure 23. Standard natural gas 40 gallon tank efficiencies under ASHRAE 90.2 and NREL/BA draw schedule.

² Due improvements to the controller board on current production, the tankless electric unit was replaced with a new one and calibrated by the manufacturer on May 27th, 2009.

shown as the average between data taken from the last reliable known months (June 2009 and October 2009). During the months of May and June 2009, we observed a noticeable decrease in efficiency with the NREL/BA draw profile. This expected outcome was similar to the other systems; however, during the month of October 2009, efficiency for both draw profiles appears to be about the same (EF = 0.49).

Tankless Natural Gas

The tankless natural gas system monthly efficiencies can be observed in Figure 24. Unlike the tank system, it has demonstrated a decrease in efficiencies during the summer months. As predicted, the short firing events in the NREL/BA profile resulted in lower efficiency for these systems. The observed decrease appears to stabilize during the month of October 2009 (COP = 0.71 ASHRAE, COP = 0.67 NREL/BA). The highest daily efficiencies measured from the tankless system appeared during three days in April 2009 reaching 80% (eff = 0.804), although efficiencies during the rest of April resulted in lower monthly values overall. Efficiency values shown on the plot include the parasitic power consumption of the tankless unit. Regardless, the tankless gas system still showed substantially higher efficiencies than the tanked gas system.

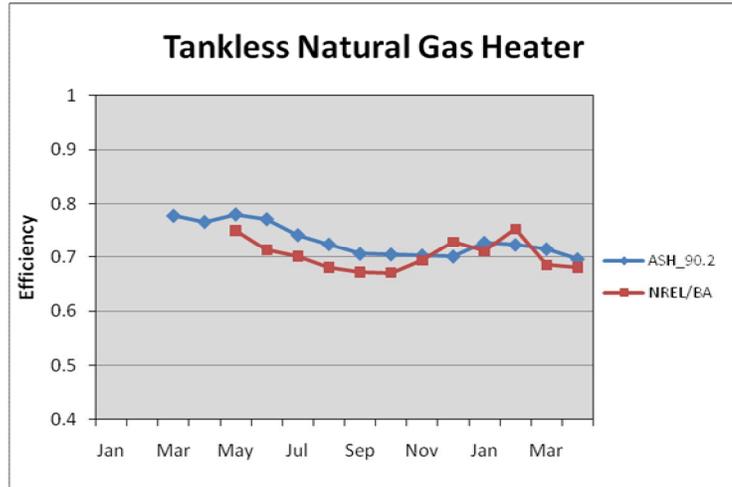


Figure 24. Average monthly efficiencies observed for the tankless natural gas system.

Flat plate Solar Systems

Unsurprisingly, solar thermal systems demonstrated the highest efficiencies during the testing period. Figures 25 and 26 show the COP efficiencies obtained through October 2009. Beginning in April 2009, where all system were submitted to a daily ASHRAE 90.2 draw profile, the solar thermal PV pumped system did not utilize auxiliary heating energy during five out of thirty days. During June, the PV pumped system demonstrated the highest efficiencies under the NREL/BA draw schedule where eight out of thirteen days auxiliary energy use was not required. Infinite COPs were often observed as shown in Figure 25.

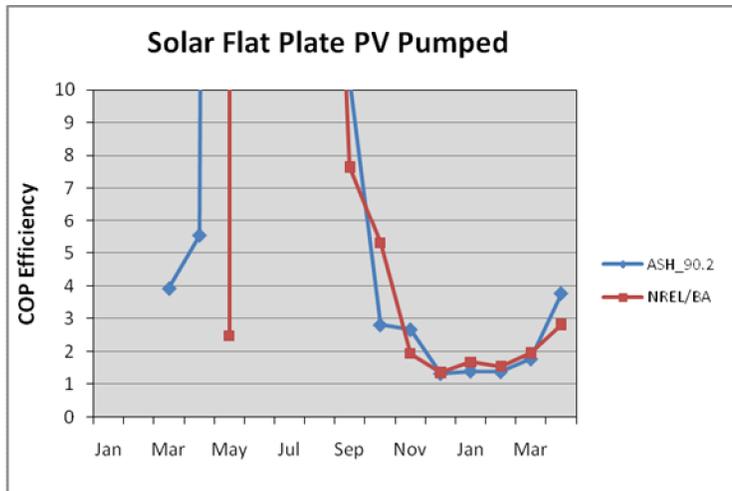


Figure 25. Average monthly efficiencies for the PV pumped solar flat plate thermal system.

On the other hand, our data also indicates that the differential control system efficiency during cloudy days exceed that of the PV pump system. This information suggests that PV pumped systems could benefit from a larger PV panel during cloudy or overcast days. We intend to evaluate this potential in future monitoring.

The effect on efficiency in the ICS and 50-gallon electric tank can be observed in Figure 27. It is evident that the NREL draw profile has an impact during most of the year, except during the winter weather where both draw profiles lower efficiencies are almost indistinguishable. A key finding of the impact on ICS performance, however, is that the NREL/BA profile has a large influence on apparent performance.

ICS Simulation Efforts

SDHW Tool (TRNSYS) Simulations Against Measured Data

Simulations were performed using the NREL solar water heating analysis tool (TRNSYS, 1994) with both the ASHRAE 90.2 and NREL/BA draw profiles. The intention was to compare results of the simulations to measured data from the ICS/50 operating in the HWS laboratory and to learn about what auxiliary energy prediction capabilities the tool can offer.

The results are shown in Figures 28 through 30. The first plot compares auxiliary energy utilized by the heating elements (4500 W) of a standard 50-gallon tank (EF = 0.91) fed by the pre-heated water of an ICS (32 ft²) system connected in series.

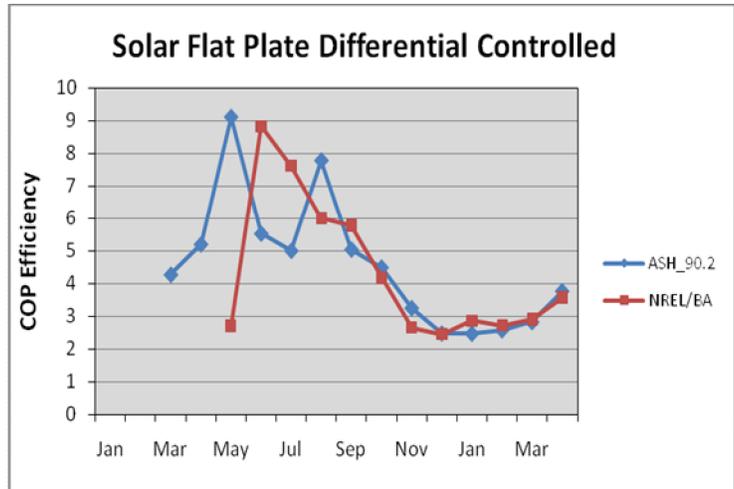


Figure 26. Average monthly efficiencies for the differentially controlled solar flat plate thermal system.

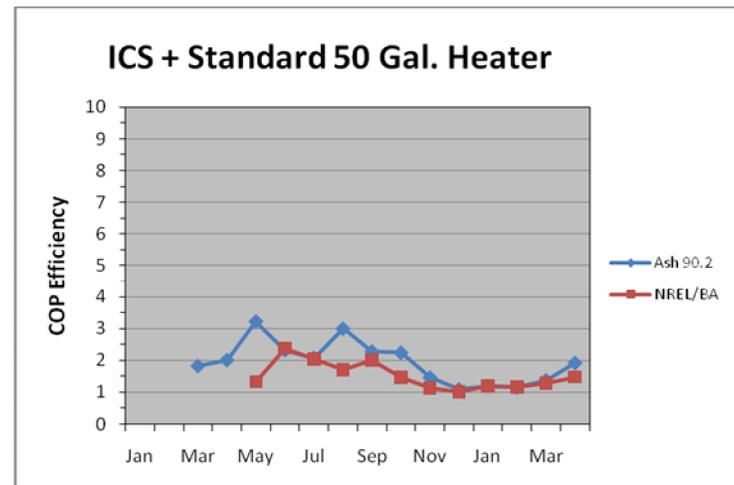


Figure 27. Average monthly efficiencies for the ICS with 50 gallon electric tank system.

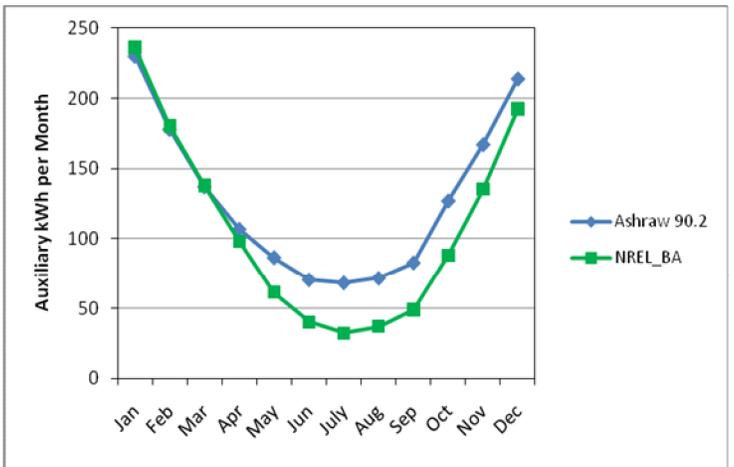


Figure 28. Comparison of NREL/BA and ASHRAE 90.2 simulations and resulting auxiliary energy used for an ICS + 50 gallon.

Results indicate a noticeable difference during the summer months where the NREL/BA requires less auxiliary energy due to smaller draws called by this profile. It is also noteworthy that the shed temperature may be affecting results that should be addressed by comparing measured values to those predicted by TRNSYS.

To evaluate the capabilities of this software, which utilizes TMY2 weather data, simulation runs were performed for both ASHRAE 90.2 and NREL/BA draw profiles compared against empirical data generated at the HWS facility. Figure 29 shows the auxiliary energy used by the ICS/50-gallon system at the HWS laboratory compared to simulation results. Fluctuations in data recorded at the HWS mostly indicate variance solar irradiance and weather data different than TMY2; however the patterns demonstrate an overall agreement in performance around the simulated curve.

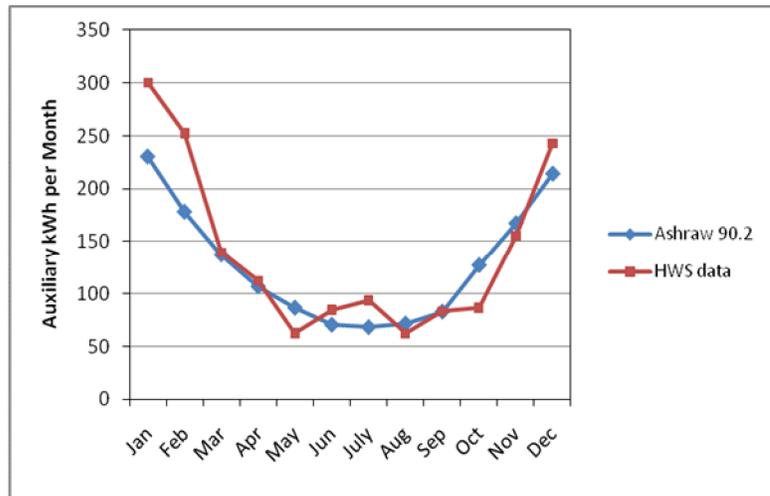


Figure 29. Auxiliary energy consumption of an ICS with 50 gallon solar system simulation vs. data recorded at HWS laboratory under ASHRAE 90.2 hot water draw schedule.

Finally, the results generated from simulations and HWS data for the NREL/BA draw pattern can be observed in Figure 30. The highest non-conforming monthly disagreement can be observed for the month of May, where actual recorded data experienced a 6 ó day period of low solar insolation. Since monthly predictions are extrapolated from only thirteen days of testing during May, deviation on the results comparing to monthly simulations are higher. Given disparities in weather data, this preliminary level of agreement is encouraging. Future analysis may use the TRNSYS model with actual weather data to further examine the level of agreement.

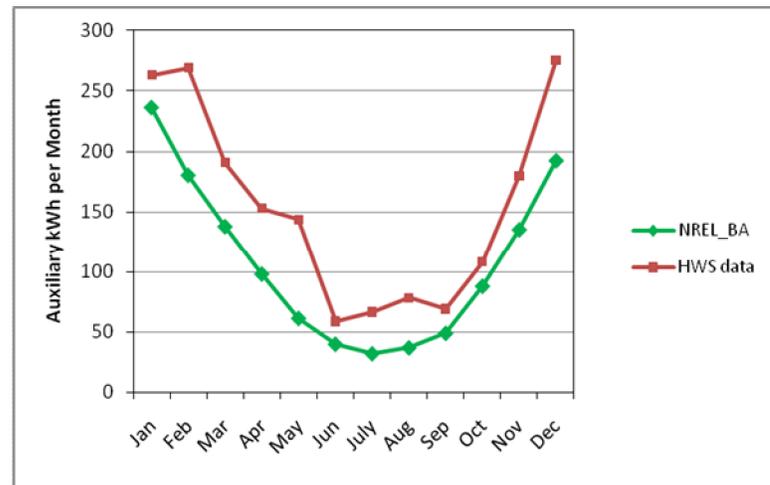


Figure 30. Auxiliary energy consumption for an ICS with 50 gallon system comparison of simulated and actual recorded data under NREL/BA draw profile.

Heat Loss Investigation on ICS Model

Data from a second data logger installed to the ICS system during May 2009 was utilized by one of our research student assistants, Camilo Gil. Thermocouples installed at the factory prior to installation of the glazing in the ICS were attached in a matrix arrangement (see Figure 30).

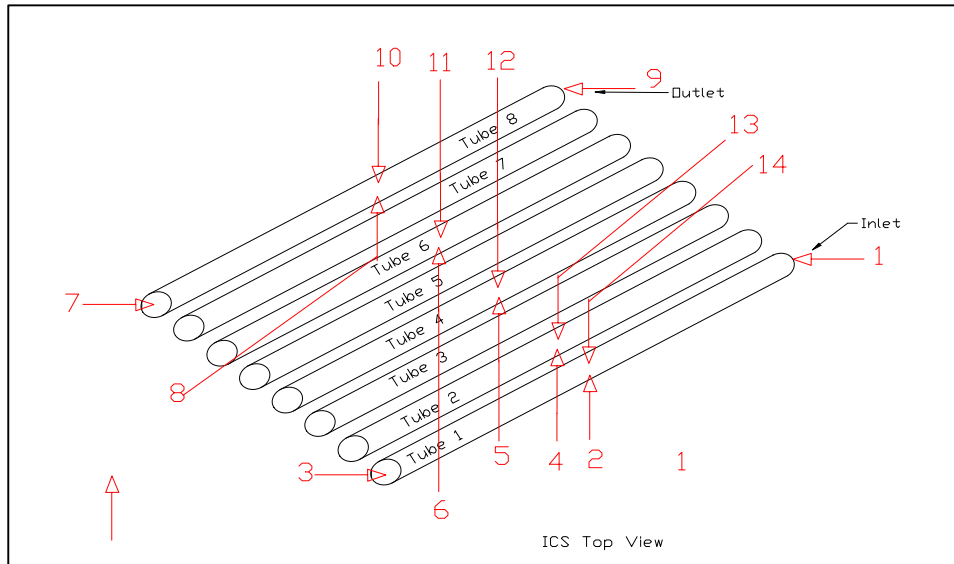


Figure 31. Matrix of thermocouples attached to an ICS for measurement of individual storage tubes.

The data collected by the second data logger, such as the one shown in Figure 32, is being used for the validation of an optimal control model that Gil created by using TRNSYS (1994).

Data shown in the plot reveals the hourly temperature distribution of the ICS system for each of the reservoir tubes. Temperatures measured at the bottom of the copper reservoir tubes are only shown in the figure. The plot illustrates the variation in temperatures on the first, second, fourth, sixth and eighth reservoirs.

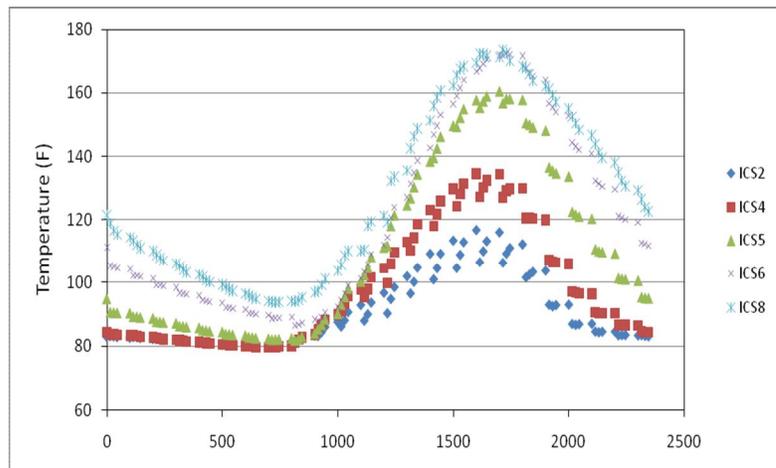


Figure 32. Temperature variation throughout the various tubes of an ICS under the ASHRAE 90.2 draw profile.

A research paper, “An Optimal Control Approach for Determination of Heat Loss Coefficient in a Domestic Water Heating System” was released for review in October 2009. The final version of this paper, available in Appendix A, was submitted to the 2010 American Control Conference - ACC2010. It will be presented in June, 2010 in Baltimore, Maryland.

Influences on Efficiency

The Hot Water Systems Laboratory has yielded high quality research data in 12+ months of operation. The efficiency plots for ASHRAE 90.2 indicate fairly good agreement with energy factor ratings published for the water heating systems tested. For example, the standard electric

water heater efficiency results indicate an overall efficiency of 0.9 during initial months; however there has been a decline in efficiency between the months of August and October 2009 (cop=0.85). Data reveals that during the months prior to August the total daily gallons draw during ASHRAE 90.2 was closer to 64 gallons per day (gpd). During October, the total amount of daily draws has diminished to 62 gpd. As a result, the efficiency drops accordingly. Unlike the ASHRAE profile, the efficiency of the water heaters under NREL/BA draw schedule appears to decrease mostly due to increased draw quantities for the same period. The tankless electric efficiency plots reveal a slight decrease in efficiency results but not as pronounced as the electric (COP from 0.93 to 0.91). Unlike the natural gas tank, with daily efficiencies approximately 0.51, the tankless gas water heater appears to be impacted where daily efficiencies were downward from 0.78 to 0.70 (ASHRAE 90.2) and 0.75 to 0.67 (NREL/BA) draw profiles, respectively.

Recommendations for Follow-up Testing

Future research should be concentrated in the investigation of very highly efficient water heating technologies. This study should include solar thermal designs with a plan to improve their performance based on testing thus far. The research advances towards reaching zero energy homes in the U.S. A key objective for anticipated testing will be to evaluate how advanced auxiliary heating systems, such as solar systems with heat pump or tankless gas backup, can be paired to provide up to 90% reduction in baseline energy use. Another important key objective of such research is to learn optimization of hybrid systems so that improved controls and algorithms can be developed. Testing would be arranged during the follow-up year with careful selection of system and components combined to provide ultra-efficiency with innovative auxiliary water heating (i.e., heat pumps or tankless gas with solar primary systems).

These systems could compare very favorably to any system presently in the market, especially when compared with the baseline standards such as electric and gas storage tanks. Testing during the second and third year of the project would examine several additional systems designed to operate in freezing climates and low-cost Integrated Collector Systems (ICS).

Based on our results, we may also develop better control of ICS system components (e.g. pipe insulation) and controls. Such projects can serve as pilot demonstrations to manufacturers in showing feasibility to achieve ultra-high energy efficiency water heating equipment for mass markets.

Conclusions and Recommendations

Simultaneous testing of seven water heating systems in the Hot Water Systems (HWS) Laboratory has led to remarkable research results. The knowledge gained from data analysis during the past year has produced a reference understanding and foundation for future comparisons of water heating systems. Continuation of this type of research is highly encouraged to investigate systems or combination of systems that can initiate higher efficiencies and also to lead the path towards future advancements in water heating appliances.

New Draw Profile (NREL/BA) and Influence on Efficiencies

Within the research at the HWS laboratory, we utilized a new residential loads methodology for testing the performance of water heating equipment. The relevancy of the evaluation results were enhanced by the utilization of alternating hot water draw schedules, ASHRAE 90.2 and a newly created schedule which we refer to as the "NREL/BA" hot water draw profile. In our view, the new draw profile represents a more realistic residential family hot water usage pattern. The NREL/BA draw profile not only provides a better representation of realistic time of day for hot water usage in a residential environment (multiple draws per hour), but it also takes into consideration the seasonal draw adjustments caused by inlet water temperature variations. It is noteworthy that although solar systems demonstrated the highest efficiencies throughout the year, the plumbing configuration utilized during testing created more challenging conditions which worked against those systems. Heat losses on the solar circulation loop are representative of a long piping run case, typical in a two-story home but longer than typical for a single-story home. Regardless, solar system outcomes were favorable.

Table 7 is a summary of ranges in efficiencies obtained throughout the 12-month period ending on April 2010. Except for the tankless systems, and in particular the natural gas tankless system, hot water system performance from testing under the ASHRAE 90.2 hot water draw profile showed COP efficiency values similar to published energy factors. On the other hand, the new NREL/BA hot water draw profile showed a slight decrease in most water heating performance when compared to results obtained with the ASHRAE 90.2 profile. Most of this decline comes from reduced hot water use, which tends to lower efficiencies.

Table 7
Averaged Profile Dependent Efficiencies Measured from Seven Water Heating Systems
HWS Lab Cocoa, FL

System	1-Year All Data (5/1/09 – 4/30/10)	ASHRAE 90.2 Draw Schedule			NREL/BA Draw Schedule		
		Min. COP	Avg. COP	Max. COP	Min. COP	Avg. COP	Max. COP
Standard Electric 50 gal. tank	0.85	0.80	0.87	0.90	0.69	0.83	0.89
Solar Flat Plate Differential w/80 gal. tank	3.41	1.94	3.55	16.3	1.93	3.29	16.03
ICS w/50 gal. tank	1.44	0.85	1.63	5.57	0.86	1.28	4.85
Solar Flat Plate PV pumped w/80 gal.	2.43	0.79	2.94	INF	0.93	2.34	7,784
Tankless Electric	0.89	0.83	0.90	0.95	0.81	0.87	0.92
Nat. Gas 40 gal. tank	0.54	0.50	0.54	0.56	0.46	0.55	0.66
Tankless Nat. Gas	0.71	0.66	0.72	0.81	0.62	0.70	0.82

The difference in efficiencies with NREL/BA draw profile is pronounced for the standard 50-gallon electric water heater during summer months, where efficiency drops below 0.8 during the months of July thru September. The efficiency reduction is primarily due to the lower quantity of water drawn (average draws below 54.84 gal/day) and the higher inlet water temperature

experienced during summer months relative to the tank losses. In general, draw profile efficiencies for water heating systems utilizing flat plate solar collectors do not appear to be affected as much by the draw profile.

However, efficiency results for the ICS with 50-gallon storage tank do show a marked difference with the NREL/BA profile. This disparity is primarily due to the greater quantity of hot water used in the NREL/BA profile in winter when ICS performance is poor. This fact is also evident in the monthly COPs for the ICS as system seen in Table 6A. The realistic nature of monitoring with the NREL/BA profile should be viewed within the context of previous monitoring efforts. For instance, the Solar Weatherization Assistance Program (SWAP) completed in the mid-1990s showed a derived average FEF (Florida Energy Factor) from measured system performance of 1.68 for the 19 ICS systems with a solar fraction of 45% (Harrison and Long, 1998). This result compared to 2.52 for the 15 standard flat-plate systems with a solar fraction of 64%. Most of the ICS systems were of similar configuration to the PT40s being tested at the HWS. Many of the flat plate collectors were 32 sqft AE-32 type units. Thus, the SWAP results showed a greater disproportion between flat plate and ICS systems than TRNSYS predicted via simulation. Not surprisingly, the SWAP data is very closely aligned with measured results from the HWS lab.³

Natural gas systems also demonstrated a slight difference in efficiency due to the alternate draw profile but not nearly as pronounced as the electric based systems. Furthermore, the largest system efficiency decrease observed over time was demonstrated by the tankless natural gas system. Efficiencies dropped to 70% levels under the ASHRAE 90.2 draw schedule during September 2009 and do not appear to recover to the higher initial efficiency values (COP = 0.78) as it demonstrated after initial operation when the appliance was new. Perhaps this outcome is due to the formation of scaling on the heat exchanger plates. Efficiencies for the tankless gas water heater under the NREL/BA draw profile dropped below 0.7 (Sept-Nov 2009) but did recover on par with efficiencies obtained from ASHRAE 90.2 during the three months ending on April 2010.

Although we found lower tankless gas efficiencies with more realistic draw profiles, as seen in earlier work (Davis Energy Group, 2006), this conclusion was partly offset by lower measured efficiencies by tank gas storage systems.

Average Daily Performance

The average daily energy consumption (electric and natural gas) demonstrated for the period of March 1, 2009 and April 30, 2010 can be examined on the second column of Table 8. The average daily energy consumption of 7.45 kWh/day was measured from the standard electric 50-gallon water heater. Nonetheless, this quantity varies from 7.88 kWh/day for the ASHRAE profile versus 7.07 kWh/day for the more realistic NREL/BA profile. For analytical purposes, this daily average value is considered to be a baseline to which all other electric systems are compared.

³ We also speculate that if the ICS system is configured similar to the flat plate solar systems with a single-element storage tank, it could yield higher efficiencies and lower daily auxiliary energy used. Another mechanical design change alternative would be to include a form of smart control to limit or delay of the activation of auxiliary heating during morning hours until the ICS energy is replenished. This strategy would fall under the category of smart controls and would be highly recommended for ICS systems plumbed in series with standard electric tanks.

As expected, the highest energy reductions are demonstrated by the solar thermal systems, particularly flat plate collectors. Surprisingly, the flat plate solar systems do not appear to be affected substantially by the NREL/BA draw profile schedule. The result is an average daily difference of only 200 watt-hours or less per day.

Table 8
Average Daily Energy Consumption for Hot Water Systems
(May 1, 2009 ó Apr 30, 2010)

System	Daily Average Consumption All data days (N=365)	Daily Average Consumption ASHRAE 90.2 Draws (N=166)	Daily Average Consumption NREL/BA Draws (N=174)
Standard Electric 50 gal. Tank	7.45 kWh/day	7.88 kWh/day	7.07 kWh/day
Solar Flat Plate Differential w/80 gal. tank	2.84 kWh/day	2.94 kWh/day	2.74 kWh/day
ICS w /50 gal. tank	4.99 kWh/day	4.79 kWh/day	5.21 kWh/day
Solar Flat Plate PV pumped w/80 gal.	2.96 kWh/day	3.09 kWh/day	2.87 kWh/day
Tankless Electric	7.00 kWh/day	7.34 kWh/day	6.71 kWh/day
Nat. Gas 40 gal. tank	39.1 cu. ft/day (Nat. Gas)	40.0 cu. ft/day (Nat. Gas)	38.3 cu. ft/day (Nat. Gas)
Tankless Nat. Gas	29.2 cu. ft/day (Nat. Gas)	30.6 cu. ft/day (Nat. Gas)	28.0 cu. ft/day (Nat. Gas)

Further analysis was performed by separating the alternate draw event periods for ASHRAE90.2 and NREL/BA profiles. Interesting influences on energy savings were discovered. Lower average daily electric consumption of the reference standard 50-gallon electric system is seen on days that utilize the NREL/BA draw schedule. Since absolute daily energy consumption is lower, the available energy savings for competing technologies will be less than those obtained from the ASHRAE 90.2 schedule.

Based on the dependent draw profile results shown in Table 8, an average demand reduction was calculated as compared to the standard electric reference system. Results are shown in Table 9A and 9B for all solar systems which utilize electric auxiliary and also for the tankless electric. As expected from the results shown, any of these systems provide an energy reduction when compared to the electric reference standard 50-gallon heater. Nevertheless, the ICS/50 gallon system demonstrated that it is strongly affected by the draw profile.

Table 9A
Average Daily Electric Reduction for Solar Systems and Tankless
Electric as Compared to the Standard Reference Electric 50-Gallon Water Heater
Under Two Hot Water Draw Profiles

	ASHRAE 90.2	NREL/BA	Change
Solar Flat Plate Differential w/80 gal. tank	62.7%	61.2%	-1.5%
ICS w /50 gal. tank	39.2%	26.3%	-12.9%
Solar Flat Plate PV pumped w/80 gal. tank	60.7%	59.4%	-1.4%
Tankless Electric	6.9%	5.0%	-1.9%

Table 9B
Average Daily Natural Gas Reduction for the Tankless System as Compared to the
Standard Reference 40-Gallon (NG) Water Heater Under Two Hot Water Draw Profiles

	ASHRAE 90.2	NREL/BA	Change
Tankless Nat. Gas	23.5%	26.9%	+3.4

In examining the results, we find that the BA/NREL profile for a standard electric resistance water heater (7.07 kWh day) at 2,580 kWh is very close to what FSEC measured with *Progress Energy* in 150 electric resistance heaters in 1999 (2,325 kWh) (Masiello and Parker, 2004). Our results are likely higher because hot water consumption is perhaps even lower than the 54.8 gallons per day in the BA/NREL profile. This difference was underscored recently in data presented by Martin Thomas at the from *Natural Resources Canada* (Thomas, 2010) which showed 37 homes in Ontario with measured average annual hot water volumes of only about 196 liter or 50 gallons per day. This data comes from a cold location with low ground water temperatures which would suggest the numbers should not be greater in Florida.

Summary of annual reductions for systems using the more realistic NREL/BA profile:

- A standard electric tank (EF = 0.91) showed an average COP of 0.82.
- A standard natural gas tank (EF = 0.59) showed an actual COP of 0.52.
- Flat plate with either differential control or PV pumping saved 61% and 59% of baseline energy, respectively.
- ICS system saved 26% of water heating energy (COP averaged 1.51).
- Tankless electric saved only 5% of water heating energy (COP averaged 0.87).
- Tankless gas (EF = 0.83) saved 27% of water heating energy relative to the standard natural gas tanked system (COP = 0.70).

Detailed findings from our research:

- The PV flat plate system does not appear to be circulating sufficiently on cloudy days and consequently suffers in efficiency particularly in winter. This result will be researched in 2010-2011 by supplementing the PV pumping with a larger wattage PV panel.

- The ICS system shows much lower reductions with the BA/NREL profile since more hot water is needed in winter and less in summer. Performance of the ICS system varies inversely as a result, and operation is worse in winter and better in summer. Thus, the percent electrical reduction is 39% for an ICS system with the 90.2 profile and only 26% with the BA/NREL profile.⁴ We expect to study possible performance enhancements in 2010 thru 2011.

Our research has also provided insight into why the TRNSYS simulation may have been over-predicting ICS performance relative to that measured in the field. The over prediction results because its performance is very strongly impacted by the seasonal nature of hot water draw profile. However, our results from the research combined with empirical field data indicate that the BA/NREL profile is more realistic relative to monitored data and likely better reflects typical homeowner conditions. Using variations in draw volume with season, TRNSYS and other simulations should provide a more representative prediction of results. This is particularly important with systems, such as ICS solar systems or heat pump water heaters, where heating performance itself is strongly tied to changing outdoor thermal conditions.

⁴ It has been suggested that the shortfall in performance is due to the use to both an upper and lower element in the ICS auxiliary tank. While this may be an influence in the overall performance of the system, it does not account for the clear fact that the ICS system performs much more poorly in winter months when water heating loads are higher and shown in the difference in performance under the two draw profiles. However, we do plan to evaluate the impact of disabling the lower element in testing of the ICS system in the second year.

References

- ANSI/ASHRAE Standard 90.2-1993. Energy Efficient Design of Low-Rise Residential Buildings, Section 8.9.4, "Hourly Domestic Hot Water Fraction" and Table 8-4, "Daily Domestic Hot Water Load Profile", pp 53-54. American Society of Heating, Refrigerating and Air Conditioning Engineers, Atlanta, GA.
- Becker, B.R. and Stogsdill, K.E., 1990. "Development of Hot Water Use Data Base," ASHRAE Transactions, Vol. 96, Part 2, pp. 422-427. American Society of Heating, Refrigerating and Air Conditioning Engineers, Atlanta, GA.
- Bouchelle, M.P., Parker, D. S. and Anello, M., 2000. "Factors Influencing Water Heating Energy Use and Peak Demand in a Large Scale Monitoring Study." *Proceeding of the Symposium on Improved Building Systems in Hot Humid Climates*, Texas A&M University, College Station, TX.
- Cromer, C.J., 1984. *The Effect of Circulation Control Strategies on the Performance of Open Loop Solar DHW Systems*, Florida Solar Energy Industry News, June.
- Davis Energy Group, 2006. *Field And Laboratory Testing of Tankless Gas Water Heater Performance*, Report prepared for the California Energy Commission, April.
- DeOreo, W. D. and Mayer, P. W., 2000. The End Users of Hot Water In Single Family Homes from Flow Trace Analysis, Aquacraft Inc. Report, undated.
- Harrison, J. and Long, S., 1998. Solar Weatherization Assistance Program, Final Report, prepared for the FL Dept of Community Affairs, Florida Solar Energy Center, FSEC-CR-1028-98, Cocoa, FL, August.
- Hendron, R and Burch, J., 2007. "Development of Standardized Domestic Hot Water Event Schedules for Residential Buildings," NREL/CP-550-40874, Energy Sustainability, Long Beach, CA, June 27-30, 2007.
- Hoeschele, M. A. and Springer, D., 2008. "Field and Laboratory Testing of Gas Tankless Water Heater Performance" ASHRAE Transactions, Vol. 114, Part 2, pp. 453-461. American Society of Heating, Refrigerating and Air Conditioning Engineers, Atlanta, GA
- Ohno, H., Mano, T., Nishina, D. and Kawano, N., 2000. "The Preferred Shower Temperatures with Post-shower Physiological and Subjective Responses for Young Females in Summer and Winter Experiments," Journal of the Human-Environment System, Vol. 4, pp. 61-68.
- Lowenstein, A. and Hiller, CC., 1996. "Disaggregating Residential Hot Water Energy Use," ASHRAE Transactions, pp. 1019-1026.

- Masiello, J. and Parker, D., 2002. Factors Influencing Water Heating Energy Use and Peak Demand in a Large Scale Residential Monitoring Study, Vol. 1, American Council for an Energy Efficient Economy, Washington D.C.
- Merrigan, T., 1983. Residential Conservation Demonstration: Domestic Hot Water, Final Report, FSEC-CR-90-83, Florida Solar Energy Center, Cocoa, FL.
- Merrigan, T.J., 1988. "Residential Hot Water Use in Florida and North Carolina." ASHRAE Transactions, Vol. 94, Part 1.
- Merrigan, T. and Parker, D., 1991. "Electrical Use, Efficiency, and Peak Demand of Electric Resistance, Heat Pump, Desuperheater, and Solar Hot Water Heating Systems," Proceedings of the 1990 Summer Study on Energy Efficiency in Buildings, Vol. 9, p. 221, American Council for an Energy Efficient Economy, Washington D.C.
- Parker, D.S., 2002. "Research Highlights from a Large Scale Residential Monitoring Study in a Hot Climate." *Proceedings of International Symposium on Highly Efficient Use of Energy and Reduction of its Environmental Impact*, pp. 108-116, Japan Society for the Promotion of Science Research for the Future Program, Osaka, Japan.
- Perlman, M, and B.E. Mills, 1985. "Development of Residential Hot Water Use Patterns." ASHRAE Transactions, Vol. 91, Part 2A, pp. 657-679. American Society of Heating, Refrigerating and Air Conditioning Engineers, Atlanta, GA.
- Pratt, R.G., et al., 1989. Description of Electric Energy Use in Single-Family Residences in the Pacific Northwest, End-Use Load and Consumer Assessment Program (ELCAP), Pacific Northwest Laboratory, DOE/BP-13795-21, Richland, WA, April 1989.
- Thomas, M., 2010. "More Information on Hot Water Use in Canada," Natural Resources Canada, the 2010 ACEEE Hot Water Forum, May 12-14th 2010, Ontario, CA.
- "TRNSYS, A Transient Simulation Program," 1994. Solar Energy Laboratory, University of Wisconsin, Madison, WI.

Appendix A

An Optimal Control Approach for Determination of the Heat Loss Coefficient
in a Domestic Water Heating System

An Optimal Control Approach for Determination of the Heat Loss Coefficient in a Domestic Water Heating System

Camilo Gil, Michael Haralambous, *Member, IEEE*, Zhihua Qu, *Fellow, IEEE*
and Marwan Simaan, *Fellow, IEEE*

Abstract— Integral collector storage (ICS) solar domestic water heating systems are an alternative to help meet the hot water energy demands in a household. In order to evaluate the potential benefits and contributions from the system, it is important to be certain that the modeling scheme is as accurate as possible. The overall heat loss coefficient (U_{loss}) plays an important roll in such a scheme and in the performance prediction methodology of the ICS. This paper presents the results of an investigation of the application of optimal control theory to find how U_{loss} varies with time, for a particular non-concentrating ICS system. The time-varying U_{loss} obtained was used in a proposed model, and the resulting simulated ICS performance was compared to the real measured performance and the simulated case when U_{loss} was time-invariant. After comparison, it was determined that the use of a time-varying U_{loss} in the modeling scheme significantly improves the ICS performance prediction.

I. INTRODUCTION

Integral collector storage (ICS) solar water heaters are passive systems which combine thermal storage and solar collection functions in a single unit. They are usually roof-or ground-mounted. In these systems, mains water is used as the heat collecting fluid and they require neither pumps, control valves, sensors, heat exchangers, control units nor electrical components. Instead, they only require local water pressure and solar radiation to operate and, in most applications, they function as a pre-heater to a conventional water heater. There exist several different designs and configurations for ICS systems, but in this study we focus specifically on one of them. In the design of interest, the fluid is stored in eight (8) copper tubes that are connected (welded) in series so that the outlet of one tube feeds the inlet of the next one. Physically, the tubes are arranged in a parallel fashion and placed within a collector enclosure. Figure 1 shows the basic diagram for this configuration.

The collector/storage device absorbs solar radiation and raises the temperature of the water stored in the tubes

This work is sponsored by the U.S. Department of Energy (DOE), Office of Energy Efficiency and Renewable Energy, Building America Program under cooperative agreement number DE-FC26-06NT42767. The authors appreciate the support of Subrato Chandra and Carlos Colon for leading the experimental research at the Florida Solar Energy Center.

The authors are with the University of Central Florida, Orlando, FL 32816. Camilo Gil is with the Florida Solar Energy Center and the School of Electrical Engineering and Computer Science and Michael Haralambous, Zhihua Qu, and Marwan Simaan are with the School of Electrical Engineering and Computer Science. (Corresponding author, C. Gil, e-mail: cgil@mail.ucf.edu).

(tanks). The objective is to maximize solar radiation collection while minimizing thermal loss. Then, the unit is well insulated for increased heat retention and to reduce heat losses to ambient, especially at night and non-solar radiation collection periods. Additionally, in order to maximize solar radiation collection while minimizing thermal loss, the ICS in this study has a double-glazed optical cover system, glazing gaskets, selective surface coating and closed cell foam. Table I shows the basic system specifications.

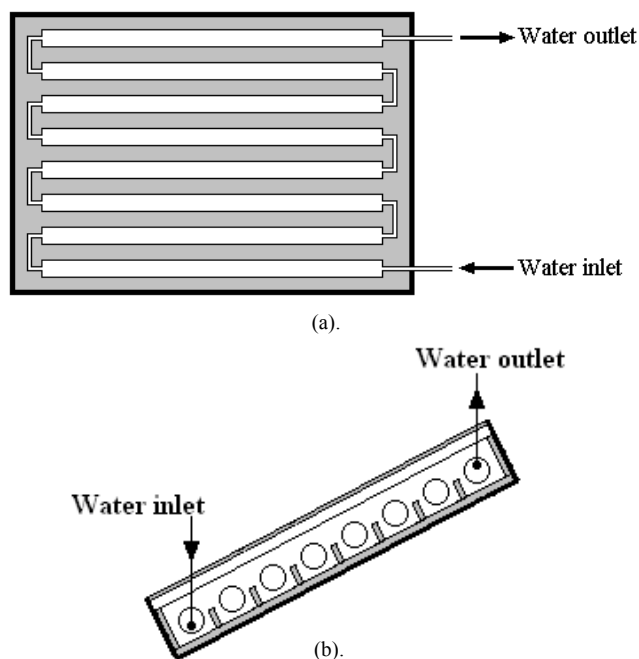


Fig. 1. ICS diagram. a) Top view. b) Side view

TABLE I. ICS SYSTEM SPECIFICATIONS

Cover area	2.77 m ²
Tilt	27°
Azimuth	180°
Volumetric capacity	0.1567 m ³

When the tops of the absorber tanks completely fill the aperture area, the ICS unit is called non-concentrating. When internal reflectors concentrate solar radiation to an absorber tank within the enclosure, the ICS is called concentrating ICS unit. As seen from the previous

description, the system of interest is a non-concentrating ICS unit.

Water heating itself accounts for a significant portion of the total annual energy consumption in a regular home, and solar domestic water heating is an attractive alternative to help meet the hot water energy demands. In order to evaluate the potential benefits and contributions from the ICS, it is important to be certain that the modeling scheme is as accurate as possible.

The overall heat loss coefficient (U_{loss}) plays an important roll in such a scheme and in the performance prediction methodology of the ICS. Thus the efforts described in this paper mainly concentrate on the investigation of how U_{loss} varies with time and its influence in the performance prediction of the ICS. The energy delivered by the system was simulated using a time-varying and a constant U_{loss} and then these results were compared to the measured amount of energy delivered.

As it will be shown in this paper, the use of a time-varying U_{loss} in the simplified modeling scheme would significantly improve the performance prediction over the conventional case where U_{loss} is assumed to be time-invariant.

The analysis described in this paper is based on optimal control theory, and the obtained results are compared with actual monitored data from the ICS at the Florida Solar Energy Center (FSEC).

Control methodologies have been previously applied to water heating and solar systems problems in different ways. Prud'homme and Gillet [1] segmented the auxiliary heater in a solar kit and developed an advanced control strategy that led to improvements in terms of comfort and energy consumption. Oestreicher, Bauer and Scartezzini [2] developed and installed a prototype predictive controller in a non-residential building where solar and free gains supply more than 50 % of its heating energy during winter. The controller determines the heat to supply for the next hour in order to optimize comfort and minimize energy consumption over a 24-hour period. A similar work was performed by Williamsons, Danaher and Craggs [3]. Camacho, Berenguel and Rubio [4] implemented an application of generalized predictive controllers to the distributed collector field of a solar power plant where algorithms based on gain scheduling and nonlinear prediction are used. It was shown that this approach seems to be an effective way of dealing with long range controllers for non-linear processes. Other applications for solar power plants have been developed by Johansen, Hunt and Petersen [5], and Pickhardt and Neves da Silva [6].

II. MODELING AND SIMPLIFIED DYNAMICS

There are many heat transfer processes in the ICS system [7]. However, an analytical solution of the model is usually available only for an idealized system. Numerical solutions or experiments may be used to empirically quantify the non-

ideal aspects of the physical problems that were avoided in the analytical solution.

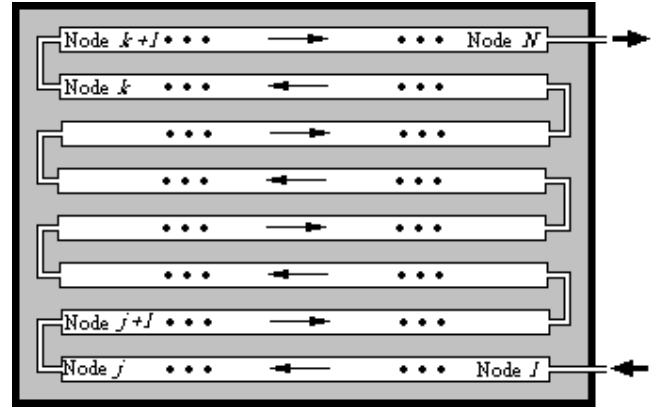


Fig. 2. ICS storage divided into N isothermal nodes.

When the water in each segment (node) of the storage tanks of an ICS unit is at a uniform temperature, there is no thermal stratification in the node, and the storage in such a node is termed “fully mixed”. If a set of fully mixed nodes is considered (see Figure 2), an instantaneous energy balance may be written about each node which equates the change in tanks internal energy with the absorbed solar radiation less losses to ambient and delivered energy to the adjacent node (or the conventional water heater in the case of the last node). The energy balance is expressed in equation (1) [8].

$$\frac{M_w c_p}{N} \frac{dT_n}{dt} = \frac{G_{tilt} A_c \tau \alpha}{N} - \frac{U_{loss} A_c}{N} (T_n - T_a) - m_{del} c_p (T_n - T_{n-1}) \quad (1)$$

The description of the variables used is shown in Table II.

TABLE II. ICS VARIABLES DESCRIPTION

M_w	mass of water in the ICS system tanks (kg)
c_p	specific heat of water (4186 J / kg·°C)
N	number of nodes in the ICS (unitless)
n	node number (1... N)
dT_n/dt	rate of change in the node water temperature (°C / s)
G_{tilt}	solar radiation on a tilted surface (W / m ²)
A_c	aperture area (m ²)
$\tau \alpha$	transmittance-absorptance product (unitless)
U_{loss}	overall heat loss coefficient (W / m ² ·°C)
T_n	node water temperature (°C)
T_a	ambient temperature (°C)
m_{del}	draw flow rate through the ICS unit (kg / s)

The quantity $M_w c_p / N$ represents the thermal mass (heat capacity) of the water in each node; the heat capacity of the ICS unit itself is neglected. In reality, the system presents

top, back, and edge losses separately; however, only one overall heat loss coefficient, U_{loss} , is included in the model. Typically U_{loss} is assumed to be time-invariant for modeling purposes [8-10]. This coefficient will play an essential roll in the development of this paper. Figure 3 shows a simplified block diagram of the ICS system with T_m representing mains water temperature measured in degrees Celsius.

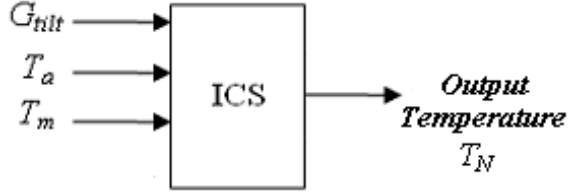


Fig. 3. Simplified ICS block diagram.

III. OPTIMAL CONTROL THEORY AND TIME-VARYING U_{Loss}

The assumption that U_{loss} is a constant value is currently used in nowadays calculations regarding ICS systems performance prediction. However, in reality U_{loss} is time-varying and it is desired to know how it varies. The heat loss coefficient changes over time because it depends on the operating condition of the system. In other words, U_{loss} is a function of the state T . This will be visualized later in the simulations section. Before getting to the details of how to accomplish this task, the formulation proposed in equation (1) is modified taking into account the following considerations.

$$\begin{aligned} x &= T \\ u &= b_2(t) \\ A &= f(b_3(t)) \\ B &= g(\mu_2(t)) \\ v &= h(b_1, \mu_1(t), b_3(t), \mu_3(t)) \end{aligned}$$

Here,

$$b_1 = \frac{A_c \cdot \tau \alpha}{M_w \cdot c_p}, \quad b_2(t) = \frac{A_c \cdot U_{loss}(t)}{M_w \cdot c_p}, \quad b_3(t) = \frac{N \cdot m_{del}(t)}{M_w}$$

$$\mu = \begin{bmatrix} \mu_1(t) \\ \mu_2(t) \\ \mu_3(t) \end{bmatrix} = \begin{bmatrix} G_{filt}(t) \\ T_a(t) \\ T_m(t) \end{bmatrix}$$

Equation (2) shows the resulting system.

$$\dot{x} = A(t)x + B(t)u - xu + v(t) \quad (2)$$

Equation (2) describes a non-linear time-varying system with known disturbances, where U_{loss} became the input to the system. According to this formulation and the objective of finding how U_{loss} varies with time, the problem can now be analyzed using optimal control theory. Here, it is desired to find the minimal value of the input u such that the system follows a desired or reference output r . Such a nominal output is obtained from the actual measured values of the system at the Florida Solar Energy Center. Before formulating the optimal control approach, an extended Kalman estimator was implemented to obtain U_{loss} without satisfactory results. It is important to note that in the input u to be found would be reflected the aspects of the physical problem that were avoided in the presently available modeling scheme. Figure 4 shows a simplified block diagram of the resulting system.

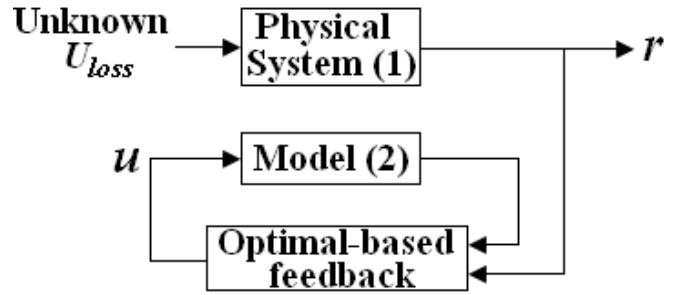


Fig. 4. ICS modified block diagram with optimal-based feedback.

In the specific case of this research, the reference data and the variables of interest are sampled and stored every 12 seconds. Then, the data for each variable are averaged every 15 minutes and this is the value for a given variable for that 15-minute interval. It is desired to solve the above mentioned problem for each interval. According to this, the following performance index is proposed:

$$J(t_i) = \frac{1}{2} (x(t_{i+1}) - r(t_{i+1}))^T (x(t_{i+1}) - r(t_{i+1})) + \frac{1}{2} \int_{t_i}^{t_{i+1}} R \cdot u^2(t) \cdot dt \quad (3)$$

where $i = 0, 1, 2, \dots, 95$ and $i = 0$ is midnight and $t_{i+1} - t_i$ corresponds to 15 minute intervals.

Here $R > 0$ and the desired final-state value $r(t_{i+1})$ is given. Thus, we want to find the control $u(t)$ over the interval $[t_i, t_{i+1}]$ to minimize $J(t_i)$. Then, we must solve the state equation (2), the co-state equation (4) and the stationarity condition (5).

$$-\dot{\lambda} = (A^T - Iu)\lambda \quad (4)$$

$$0 = Ru + (B - x)^T \lambda \quad (5)$$

Solving for u in (5), we get

$$u = -\frac{1}{R}(B-x)^T \lambda. \quad (6)$$

The input can be eliminated in the state and co-state equations, obtaining the Hamiltonian system given by Equations (7) and (8).

$$\dot{x} = Ax - \frac{1}{R}B(B-x)^T \lambda - \frac{1}{R}x(B-x)^T \lambda + v \quad (7)$$

$$-\dot{\lambda} = (A^T + I(R^{-1}(B-x)^T \lambda))\lambda \quad (8)$$

The Hamiltonian system is a nonlinear ordinary differential equation in $x(t)$ and $\lambda(t)$ with split boundary conditions given as follows.

N initial conditions: $x(t_i)$ specified.

N final conditions (p conditions plus $N-p$ conditions):

p conditions given by the fixed final state function ψ .

$$\psi[x(t_{i+1})] = \begin{bmatrix} x_1(t_{i+1}) - r_1(t_{i+1}) \\ \vdots \\ x_p(t_{i+1}) - r_p(t_{i+1}) \end{bmatrix} = 0$$

Here, the values for $r_1(t_{i+1}), \dots, r_p(t_{i+1})$ are specified.

$N-p$ conditions given by λ_j .

$$\lambda_j(t_{i+1}) = \left(\frac{\partial \phi}{\partial x_j} \right)_{t=t_{i+1}} = x_j(t_{i+1}) - r_j(t_{i+1})$$

Here, ϕ is the final weighting function given below and $j = p+1, \dots, N$.

$$\phi(x(t_{i+1})) = \frac{1}{2}(x(t_{i+1}) - r(t_{i+1}))^T (x(t_{i+1}) - r(t_{i+1}))$$

The Hamiltonian system is solved numerically by using the principles of the neighboring extremal methods [12, 13]. These methods are known for obtaining nominal solutions that result in approaching the boundary conditions, and that satisfy the optimality conditions, the state and co-state equations. After solving the Hamiltonian system it can be determined how U_{loss} varies with time.

IV. MEASURED VARIABLES

An ICS system has been installed at FSEC where ambient and other variables are being monitored and stored permanently. The following figures show the variables taken into account in the analysis. These values were measured during a 24 hour period on May 5th, 2009 in Cocoa, FL.

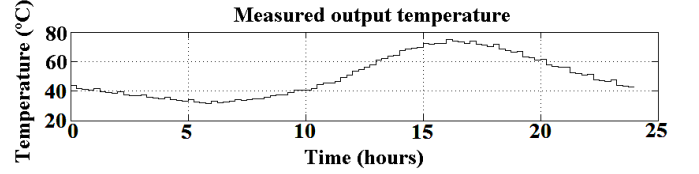


Fig. 5. ICS measured output temperature.

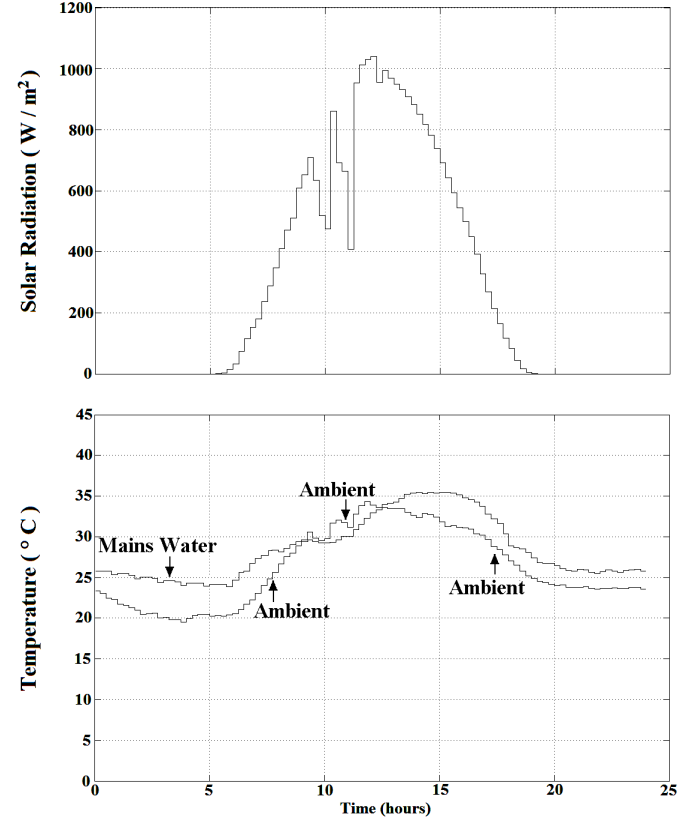


Fig. 6. Ambient conditions.

Figure 7 shows the instantaneous water draw flow rate through the ICS for a 24 hour period. The amount of hot water drawn each hour is more easily visualized on Figure 8 which shows the cubic meters draw.

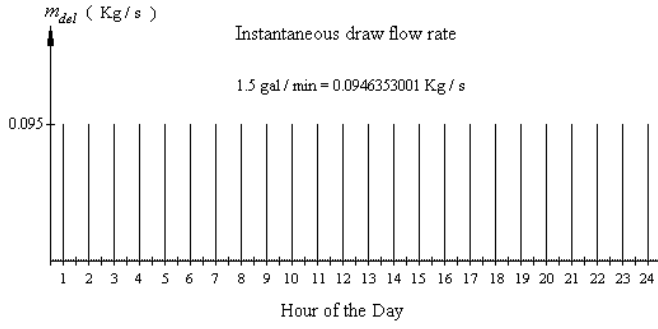


Fig. 7. Instantaneous hot water flow rate.

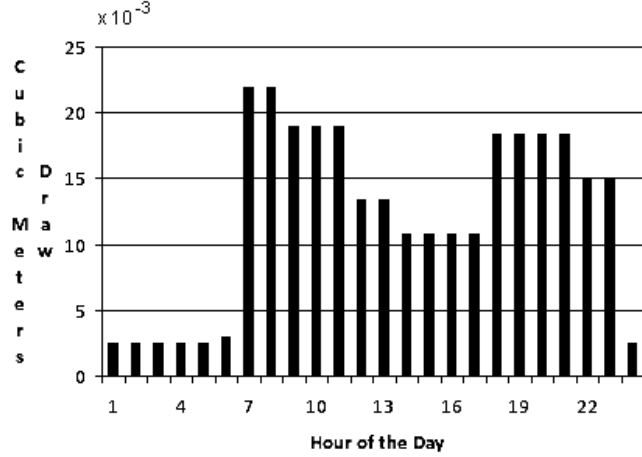


Fig. 8. ASHRAE 90.2 hot water draw profile [14-16].

V. SIMULATIONS

Simulations using MATLAB/Simulink were performed in order to find U_{loss} , where an extremal neighboring method was implemented to solve the resulting Hamiltonian system. The obtained U_{loss} value is shown in Figure 9.

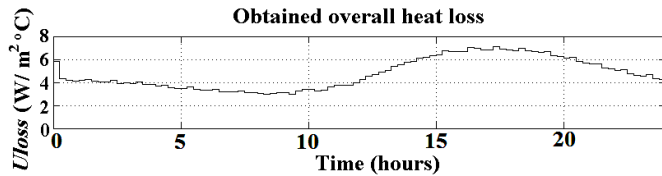


Fig. 9. Obtained U_{loss} .

MATLAB/Simulink was also used to simulate the output of the ICS using the modeling scheme in equation (1). First, the system was simulated with the obtained time-varying overall heat loss coefficient. Then, the system was simulated with the constant U_{loss} . The constant value for U_{loss} was obtained from standards established by the Solar Rating and Certification Corporation (SRCC) and others [11]. The results of the simulations are illustrated on Figures 10 and

11. By comparing Figures 9 and 10, it can be seen that a relationship between U_{loss} and the state T exists.

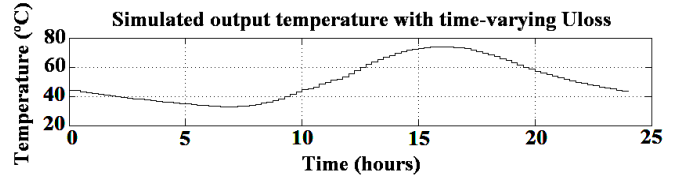


Fig. 10. Simulated output temperature with time-varying U_{loss} .

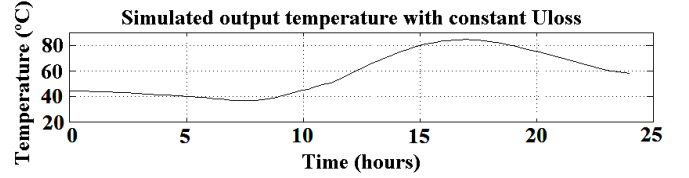


Fig. 11. Simulated output temperature with constant U_{loss} .

At a first glance, all figures of the output temperature (Figures 5, 10 and 11) look similar. However, note that the final value obtained using a time-varying U_{loss} tends to the measured final value. This is not the case when using a constant U_{loss} . Figure 12 shows the output temperature for all three cases.

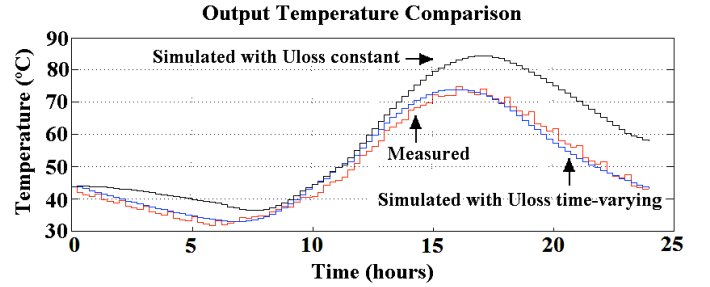


Fig. 12. Simulated and measured output temperature.

In order to compare the obtained performance, it is worth determining the amount of energy delivered in all three cases (i.e. measured value, simulation with U_{loss} time-varying, and simulation with U_{loss} constant) for a 24 hour period.

The amount of energy in Watt-hour (Wh) delivered during a given interval is given by Equation (9).

$$Q_{del} = \frac{1}{3600} \cdot m \cdot c_p \cdot (T_N - T_m) \quad (9)$$

Here,

- m = mass of released water (kg)
- c_p = specific heat of water (4186 J / kg·°C)
- T_N = output water temperature (°C)
- T_m = mains water temperature (°C).

Figures 13 and 14 show the instantaneous energy delivered when using time-varying and constant U_{loss} values respectively, compared to the measured value. Table III

shows the amount of energy delivered (in Wh) during a 24 hour period for all three cases.

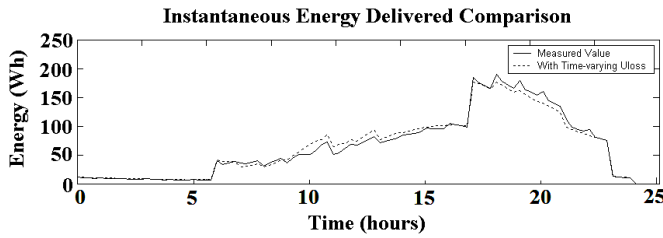


Fig. 13. Measured and simulated instantaneous energy delivered with the obtained U_{loss} .

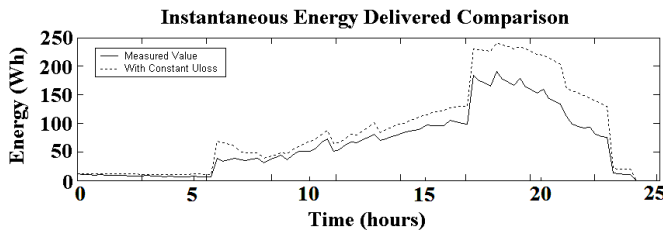


Fig. 14. Measured and simulated instantaneous energy delivered with constant U_{loss} .

TABLE III. ICS SYSTEM ENERGY DELIVERED COMPARISON

Measured Value	Time-varying U_{loss}	Constant U_{loss}
6417 Wh	6866 Wh	8725 Wh

By comparing the measured value with the other two cases, it can be seen that the delivered energy obtained with constant U_{loss} is 35 % higher than the measured value, while the value obtained with varying U_{loss} is less than 7% higher. This represents a significant improvement over the conventional case with constant U_{loss} .

It is important to note that the problem of finding how U_{loss} varies with time, was solved for one specific day. In general it is desired to know the ICS performance over a one year period taking into account all four seasons. Although the conventional calculated performance value (with constant U_{loss}) for one day may seem close to the real value, its difference would considerably increase over a one year period calculation.

In order to find how U_{loss} varies over a one year period using the proposed approach, and its relationship with the other variables affecting the system, additional efforts are required, including solving the resulting Hamiltonian system.

VI. CONCLUSION

The capability of the obtained time-varying U_{loss} to reduce the performance prediction error makes the optimal control approach useful for the determination of the heat loss

coefficient in an ICS system. The results of this initial work imply the potential for effective determination of U_{loss} , that takes into account the aspects of the physical system avoided in the model, and other possible values in the ICS over a one year period. This technique has a strong likelihood of offering an improvement in the overall performance prediction.

REFERENCES

- [1] Prud'homme, T., and Gillet, D., "Advanced control strategy of a solar domestic hot water system with a segmented auxiliary heater," *ELSEVIER: Energy and Buildings* 1300, 2000, pp. 1-13
- [2] Oestreicher, Y., Bauer, M., and Scartezzini, J.-L., "Accounting free gains in a non-residential building by means of an optimal stochastic controller," *ELSEVIER: Energy and Buildings* 24, 1996, pp. 213-221
- [3] Williams, I., Danaher, S., and Craggs, C., "Optimization of solar building control using predictive methodologies," *6th European Congress on Intelligent Techniques and Soft Computing, EUFIT'98*, Vol. 2, Verlag Mainz, Aachen, Germany, 1998, pp. 878-879
- [4] Camacho, E., and Berenguel, M., "Application of a gain scheduling generalized predictive controller to a solar power plant," *Proceedings of the 3rd IEEE Conference on Control Applications*, Vol. 3, Glasgow, UK, August 1994, pp. 1657-1662
- [5] Johansen, T., Hunt, K., and Petersen, I., "Gain-scheduled control of a solar power plant," *PERGAMON: Control Engineering Practice* 8, 2000, pp. 1011-1022
- [6] Pickhardt, R., and Neves da Silva, R., "Application of a nonlinear predictive controller to a solar power plant," *Proceedings of the 1998 IEEE International Conference on Control Applications*, Vol. 1, Trieste, Italy, September 1998, pp. 6-10
- [7] Smyth, M., Eames, P. C., and Norton, B., "Integrated collector storage solar water heaters," *ELSEVIER: Renewable and Sustainable Energy Reviews* 10, 2006, pp. 503-538
- [8] Zollner, A., "A performance prediction methodology for integral collector storage solar domestic hot water systems," MS Thesis, University of Wisconsin, Madison, 1984.
- [9] Christensen, C., Barker, G., and Thornton, J., "Parametric Study of Thermal Performance of Integral Collector-Storage Solar Water Heaters," *Proceedings of the Solar 2000 Conference Including Proceedings of ASES Annual Conference and Proceedings of the 25th National Passive Solar Conference*, Madison, Wisconsin, June 16-21, 2000.
- [10] Anello, M., "Comparison of Solar Hot Water Systems Simulated in EnergyGauge USA and TRNSYS 15," Florida Solar Energy Center, Cocoa, FL., November 2006.
- [11] Solar Rating and Certification Corporation (SRCC), "SRCC Document OG-300: Operating Guidelines and Minimum Standards for Certifying Solar Water Heating Systems," Cocoa, FL., June 2008.
- [12] Bryson, A., and Ho, Y., "Applied Optimal Control," Hemisphere Publishing Corporation, Washington, 1975.
- [13] Lewis, F., "Optimal Control," John Wiley & Sons, New York, 1986.
- [14] American Society of Heating, Refrigeration, and Air Conditioning Engineers (ASHRAE), "ANSI / ASHRAE Standard 90.2 -1993," "Energy Efficient Design of Low-Rise Residential Buildings", Section 8.9.4, "Hourly Domestic Hot Water Fraction" and Table 8-4, "Daily Domestic Hot Water Load Profile", Atlanta, Georgia, 1993, pp 53 - 54.
- [15] American Society of Heating, Refrigeration, and Air Conditioning Engineers (ASHRAE), "HVAC Applications Handbook," Chapter 49: Service Water Heating, pp 49.9 - 49.10, Atlanta, Georgia, 1999.
- [16] American Society of Heating, Refrigeration, and Air Conditioning Engineers (ASHRAE), "HVAC Applications Handbook," Atlanta, Georgia, 1999.